Annals of Biomedical Engineering

Evaluation of the Early In vivo Response of a Functionally Graded Macroporous Scaffold in an Osteochondral Defect in a Rabbit Model

--Manuscript Draft--

Manuscript Number:	ABME-D-15-00624R1
Full Title:	Evaluation of the Early In vivo Response of a Functionally Graded Macroporous Scaffold in an Osteochondral Defect in a Rabbit Model
Article Type:	Original Article
Keywords:	Functionally Graded; Polylactic Acid-ε-Polycaprolactone, Cartilage Repair; Integration; Neotissue formation
Corresponding Author:	Mary Murphy IRELAND
Corresponding Author Secondary Information:	
Corresponding Author's Institution:	
Corresponding Author's Secondary Institution:	
First Author:	Valerie Barron, BSc PhD
First Author Secondary Information:	
Order of Authors:	Valerie Barron, BSc PhD
	Martin Neary
	Khalid Merghani Salid Mohamed
	Sharon Ansboro
	Georgina Shaw
	Grace O'Malley
	Niall Rooney
	Frank Barry
	Mary Murphy
Order of Authors Secondary Information:	
Funding Information:	Science Foundation Ireland (IE) (09/SRC/B1794) — Dr. Mary Murphy Seventh Framework Programme (BE) (HEALTH-2007-B-223298) — Frank Barry Wellcome Trust (GB) (WTD004448) — Valerie Barron
Abstract:	Cartilage tissue engineering is a multifactorial problem requiring a wide range of material property requirements from provision of biological cues to facilitation of mechanical support in load-bearing diarthrodial joints. The study aim was to design, fabricate and characterize a template to promote endogenous cell recruitment for enhanced cartilage repair. A polylactic acid poly-ε-caprolactone (PLCL) support structure was fabricated using laser micromachining technology and thermal crimping to create a functionally-graded open pore network scaffold with a compressive modulus of 10MPa and a compressive stress at 50% strain of 8.5MPa. In parallel, rabbit mesenchymal stem cells (MSC) were isolated and their growth characteristics, morphology and multipotency confirmed. Sterilization had no effect on construct chemical structure and cellular compatibility was confirmed. After four weeks implantation in an osteochondral defect in a rabbit model to assess biocompatibility,

	there was no evidence of inflammation or giant cells. Moreover, acellular constructs performed better than cell-seeded constructs with endogenous progenitor cells homing through microtunnels, differentiating to form neo-cartilage and strengthening integration with native tissue. These results suggest, albeit at an early stage of repair, that by modulating the architecture of a macroporous scaffold, pre-seeding with MSCs is not necessary for hyaline cartilage repair.
Author Comments:	
Additional Information:	
Question	**Response**
Please state the number of words in your manuscript including references.	5654

Overall Review

"This is an important study that demonstrates that an inherent advantage of the osteochondral approach when a macroporous biomaterial is used is that pre-seeding of cells is not necessary. This may be a valuable addition to the literature, and the authors are encouraged to modify the title and abstract to reflect this point of impact/significance in the field."

Comment: The authors thank the reviewers for the positive feedback and have modified the title and the abstract to reflect their comments.

Actions:

Title: The new title of the manuscript is "Evaluation of the Early *In vivo* Response of a Functionally Graded Macroporous Scaffold in an Osteochondral Defect in a Rabbit Model"

Abstract "Cartilage tissue engineering is a multifactorial problem requiring a wide range of material property requirements from provision of biological cues to facilitation of mechanical support in load-bearing diarthrodial joints. The study aim was to design, fabricate and characterize a template to promote endogenous cell recruitment for enhanced cartilage repair. A polylactic acid poly-ε-caprolactone (PLCL) support structure was fabricated using laser micromachining technology and thermal crimping to create a functionally-graded open pore network scaffold with a compressive modulus of 10MPa and a compressive stress at 50% strain of 8.5MPa. In parallel, rabbit mesenchymal stem cells (MSC) were isolated and their growth characteristics, morphology and multipotency confirmed. Sterilization had no effect on construct chemical structure and cellular compatibility was confirmed. After four weeks implantation in an osteochondral defect in a rabbit model to assess biocompatibility, there was no evidence of inflammation or giant cells. Moreover, acellular constructs performed better than cell-seeded constructs with endogenous progenitor cells homing through microtunnels, differentiating to form neo-cartilage and strengthening integration with native tissue. These results suggest, albeit at an early stage of repair, that by modulating the architecture of a macroporous scaffold, pre-seeding with MSCs is not necessary for hyaline cartilage repair."

Major concerns:

1) In the 18 rabbits, were the left and right knees different groups? They need to be different groups, since all scaffolds were processed for the same analysis (i.e., histology), as otherwise they are not truly independent samples. If this was not done, this needs to be stated as a limitation of the study, and the "n" number must be revised (cut in half) accordingly.

Comments: The authors thank the reviewer for pointing out the fact that this information was unclear in the text.

Action: To help clarify the point further information was added to the Methods section and information regarding the limitations was added to the Discussion.

Page 12 Animal surgery – "In total 18 knees were randomly assigned into three groups, including empty defect (n=5 knees, with 6 technical replicates - one rabbit received two empty defects, one in the left knee and one in the right as a result of the randomization), cell-free constructs (n=5 knees, with 6 technical replicates - one rabbit received two cell-free constructs, one in the left knee and one in the right as a result of the randomization) and MSC-

seeded constructs (n=6 knees)."

Page 21 Discussion – "In relation to limitations of the animal study, the number of replicates is noted. Due to the randomization, one rabbit received two empty defects, one in the left knee and one in the right and another rabbit received two cell-free constructs, one in the left knee and one in the right. As shown in montage of images in the supplemental figures, there was no trend for repair in the rabbit that received an empty defect in both knees, with one knee remaining empty and the other showing evidence of tissue fill, albeit fibrous tissue formation. With respect to the rabbit that received two cell-free constructs, there is evidence of neotissue formation and chondrogenesis in both knees. The number of specimens analyzed was sufficient to compare biocompatibility and early repair, but larger numbers of rabbits, with different test groups in different knees are required for the 12-week cartilage repair proof of principle studies recommended by the International Society for Cartilage Repair (ICRS)."

2) Tissue structure looks better in the empty defect than in the material-based groups. Conclusions should be modified accordingly. Perhaps the authors could comment on future improvements to the biomaterial itself to yield improved outcomes.

Comments One of the well-known disadvantages of using a rabbit model is that rabbits exhibit spontaneous repair with evidence of fibrocartilage formation, degenerative changes and evidence of arthritis. As a result, they can be used as a control for evidence of inadequate fibrocartilage. On initial observation, the tissue structure in the empty defect at four weeks looks good, but on closer examination, the absence of collagen type II and staining for collagen type I suggests the presence of fibrous tissue. With respect to future improvements to the biomaterial itself, early indications show that the open pore structure is advantageous for bone marrow diffusion and endogenous cell recruitment. At this stage, it may be better to conduct further testing using large numbers over longer time points, which would provide more information on the repair potential rather than changing the surface chemistry, mechanical properties or degradation rate of the polymer.

Action: The text in the results section and the conclusion has been modified to include information on the tissue repair in the empty defects. With respect to future studies, further information has been added to the text to show a potential future direction for this study.

Results: Page 21 "Evidence of chondrogenesis, neo-tissue formation and integration was examined using toluidine blue staining. In the montage of images from all defects shown in the supplemental figures, fibrous tissue fill can be seen in three of the size empty defects, with the other three defects remaining empty. In comparison, four of the defects containing cell-free constructs revealed evidence of neotissue formation in and around the struts of the scaffold, with two defects appearing to remain empty. A similar trend was observed for the cell-seeded scaffolds, with only two defects appearing empty. As shown in Figure 6, lateral integration with native cartilage in the empty defect was observed to be incomplete as highlighted by the black arrow. In contrast, it can be seen that there was evidence of integration between the host tissue and the cell-free construct. At lower magnification, the scaffold appeared to be integrated at the bottom and at both sides of the

defect and lateral integration with host tissue is emphasized in the 10x representative image. Of relevance is the appearance of round, toluidine blue-positively stained cells with a chondrocytic morphology seen at 20x, suggesting that the underlying bone marrow diffused in and around the scaffold struts, resulting in early chondrogenesis. With respect to the cell-seeded construct, the sections also stained positive for toluidine blue, but there was less evidence of neo-tissue organization or integration as indicated by the black arrow."
Page 21: "On first observation, it appeared that the tissue repair in the empty defect was better than that of the scaffolds. However, on closer examination, it was seen that the repair tissue was fibrous primarily, as evidenced by the presence of collagen type I staining and the absence of collagen type II staining. Moreover, there was evidence of chondrocyte clustering and hypo- and hyper-cellularity in the repair and native tissues adjacent to the empty defect, which compared well with previous findings where fibrous tissue formation was observed in empty defects and is perhaps why empty defects, are accepted as a negative control."
Page 22: "Since the materials properties and architecture of the functionally-graded scaffold are promising, these results suggest that instead of altering the surface chemistry, mechanical properties or pore architecture as a next step, proof of principle studies such as that recommended by the ICRS with larger numbers and longer time points should be conducted as they would provide very valuable information on the repair potential."

3) It is not clear whether the histology/IHC images shown represent the 'best' or 'typical' specimens from among all samples within a given group. At the least, a supplementary figure would be advised to visualize all stains for all specimens.
Comment: The images represent typical specimens from among all samples within a given group.
Action: A supplementary figure has been added showing toluidine blue staining of all defects. Further information has been added to the results section.
Page 21 "Evidence of chondrogenesis, neo-tissue formation and integration was examined using toluidine blue staining. In the montage of images from all defects shown in the supplemental figures, fibrous tissue fill can be seen in three of the size empty defects, with the other three defects remaining empty. In comparison, four of the defects containing cell-free constructs revealed evidence of cartilaginous neotissue formation in and around the struts of the scaffold, with two defects appearing to remain empty. A similar trend was observed for the cell-seeded scaffolds, with only two defects appearing empty."

4) **Replace "subchondral" with "osteochondral" throughout the manuscript. In the methods, indicate that 1 mm in rabbits corresponds to a shallow osteochondral defect, if indeed that is the case. In addition, in observations (Results), please speak to whether the defects were deep enough to reach the marrow, and whether thus these macroporous scaffolds appeared to be 'soaking up' the underlying marrow and thus endogenous MSCs at implantation.**

Comments: The authors agree with the reviewer that the 1 mm defect is a shallow osteochondral defect and have modified the text accordingly. On observation of the images, it appears that the defects are deep enough to reach the marrow and soak up the underlying marrow and endogenous cells at implantation.
Actions: All reference to subchondral defects have been replaced with osteochondral defects as recommended by the reviewer. The Methods section was modified to show that a shallow osteochondral defect was created. The results section has also been modified to address the issue of the diffusion of the underlying marrow and endogenous MSC at implantation.
Page 12: …..” a 1mm shallow osteochondral defect was created on the medial femoral condyle using a drill with a previously sterilized 2.8mm drill bit covered with a sterile depth stop.”
Page 18: “Of relevance is the appearance of round, toluidine blue-positively stained cells with a chondrocytic morphology seen at 20x, suggesting that the underlying bone marrow diffused in and around the scaffold struts, resulting in early chondrogenesis.”

Minor concerns:
1) **Use journal format for references (superscript follows punctuation, numbered at the end in alphabetical order). List all authors in references.**
Actions: The format of the references was modified according to the journal format, with superscript following punctuation and a numbered list at the end in alphabetical order was created. All authors are listed.

2) **Intro: Tone down the statement “to fabricate 3D constructs with the physical architecture and compressive properties of native tissue”**
Comment: The intro was toned down as suggested by the reviewer and the phrase was altered.
Action: Page 7: “…..to fabricate 3D porous constructs with an open tunnel network and mechanical properties similar to those proposed by previous studies[18]”

3) PLCL: Indicate molecular weight/intrinsic viscosity and manufacturer
Action: Further details on the polymer intrinsic viscosity and manufacturer were added to the text. The molecular weight was not given on the manufacturer’s datasheet but was measured and details are shown in the supplementary figures.
Page 7: …. a 70:30 polylactic acid poly-ε-caprolactone (PLCL) copolymer with an intrinsic viscosity midpoint of 1.5 dl/g (PURASORB PLC7015, Purac-Corbion, Amsterdam, The Netherlands) was selected……..”.

4) Methods: Use Greek mu instead of writing uA for microAmps.
Action: Page 7: uA was replace by µA.

5) Mechanical testing methods – add more detail to manuscript.
a. Indicate whether done in dry or hydrated conditions
b. Indicate temperature (e.g., room temperature, 37 degC)
c. Was a tare load applied? If so, indicate the tare load.

d. Indicate that the elastic compressive modulus was obtained.
e. Compressive "strength" at 50% strain must be renamed as compressive "stress" at 50% strain. "strength" implies failure. Revise throughout manuscript, including figure legends and Fig. 1B y-axis label.
f. Explain the 'resilience value' that is reported later in the Results

Actions: Page 6 Mechanical testing – The text has been modified and information has been added regarding the test conditions, the temperature and the tare load. The term elastic modulus was included. Compressive strength was changed on page 6 and throughout the manuscript and in the figure legend. The y-axis in Figure 1B was also changed.

Page 15: The resilience value is explained, and the text has been modified accordingly, "……the PLCL constructs had a mean compressive modulus of 10 ± 1.41 MPa, a mean compressive stress at 50% strain of 8.5 ± 1.35 MPa and a mean recoverable elastic energy per unit volume that can be stored in the polymer or modulus of resilience value of 1.5 ± 0.12 MPa (Fig. 1Bii)."

6) Human cells in methods – add more detail to manuscript

a. Number of donors
b. Age, gender of donors
c. What was the tissue source of the MSCs? Bone marrow?
d. Were cells from different donors pooled?
e. Were cells obtained from a commercial source? If so, indicate company. If harvested by informed consent, please provide IRB approval information.
f. Passage number of cells?

Action: More information on the human cell was added to the methods section and includes information on the number of donors, age, gender, source, whether they were pooled and the passage number.

Page 8: "…..using human bone-marrow derived MSCs as a cell source, since the ultimate application was for human use. In brief, the MSCs at passage 3 (n=3 technical replicates from one male donor aged 24) were seeded at a density of 2 x 10^4 cells/cm^2"

7) Indicate the manufacturers (and city) of culture medium components, CFU assay reagents, immunohistochemistry supplies, etc.

Action: A sentence has been added at the beginning of the Methods section describing the source of all products. The manufacturer's details have been added to the manuscript for all cell culture components, CFU assay reagents and immunohistochemistry supplies.

8) Should "white New Zealand rabbits" be "New Zealand White rabbits"?

Action: Pages 9 and 12, white New Zealand rabbits" is replaced with "New Zealand White rabbits.

9) Rabbit marrow cells: from which bone were cells harvested? Iliac crest? Femur?

Action: Information was added to show that the rabbit MSC were harvested from the tibia.

Page 9: To assess the early repair response in vivo, MSC were obtained from the tibia of skeletally mature male (>3kg) New Zealand white rabbits (Charles River, France) (n=6).

10) Were the rabbits whose cells were harvested the same rabbits who received cartilage defects? If not, what happened to these rabbits (MSC donors, n = 6) after marrow harvest, were they euthanized? If they are the same rabbits, how was mixing/matching the cells of the six donor rabbits done with the six recipient knees?
Comment: The rabbits were not euthanized. The bone marrow was harvested from the tibia under anesthetic. These rabbits were later used for other studies and were not the same rabbits used for the cartilage repair study described in this manuscript.

11) **Immunohistochemistry method: What negative control was done for non-specific staining? E.g., primary antibody omitted? IgG isotype control?**
A primary antibody was not used. The secondary antibody only was used as a negative control and did not stain positive for either collagen type I or type II. In the case of Collagen type II, tissue adjacent to the defect stained positive and was used as a positive control, while the underlying bone stained negative. In contrast, the underlying bone stained positive for collagen type I and the adjacent tissue was negative suggesting the antibodies were specifically targeting by the antibodies.

12) Results: present error for values presented for mechanical data.
Action: The standard deviation values for the mechanical data were added to the text.
Page 15: "……the PLCL constructs had a mean compressive modulus of 10 ± 1.41 MPa, a mean compressive stress at 50% strain of 8.5 ± 1.35 MPa and a mean recoverable elastic energy per unit volume that can be stored in the polymer or modulus of resilience value of 1.5 ± 0.12 MPa (Fig. 1Bii)."

13) Rephrase: "statistical difference" should be "statistically significant difference" or simply "significant difference".
Action: Statistical difference was replaced with statistically significant difference and significant difference
Page 16. "As shown in Fig. 2Bi, Fig. 2Bii and Fig. 2Biii, there was no statistically significant difference observed in metabolic activity, cell number or normalized metabolic activity per cell number for cells grown in the presence of the PLCL construct. In contrast, a significant difference was observed in metabolic activity (Fig. 2Biv), cell number (Fig. 2Bv) and normalized metabolic activity per cell number (Fig. 2Bvi) for cells grown in conditioned medium."

14) **When indicating a statistically significant difference in the Results, be quantitative with relative comparisons (e.g., 25% larger?) and indicate a p value for the comparison.**
Action: The text was modified to include quantitative details on differences observed and p-values were indicated for comparison.
Page 16 "In contrast, a significant difference was observed in metabolic

activity (Fig. 2Biv), cell number (Fig. 2Bv) and normalized metabolic activity per cell number (Fig. 2Bvi) for cells grown in conditioned medium, where a 19% increase in metabolic activity, a 32% increase in cell number and a 26% decrease in normalized metabolic activity per cell number was observed."

15) Methods need to be provided for corresponding data the Results section on 'Tri-lineage differentiation of rabbit MSCs'. E.g., no oil red staining mentioned in methods.

Action: The methods used to provide data for the tri-lineage differential of the rabbit MSC were added:

Pages 9/10/11/12 "For adipogenesis, confluent cultures were exposed to induction medium (DMEM high glucose (HG-DMEM), 10% FBS, 1% P/S, 10µg/ml insulin, 1µM dexamethasone, 500µM isobutylmethylxanthine and 200µM indomethacin) for 3 days, followed by 1-3 days in maintenance medium (DMEM high glucose, 10% FBS, 1% P/S and 10µg/ml insulin). The cycle was repeated 3 times with cells left in maintenance medium for 7 days in total prior to harvesting for analysis. At the end of the culture period, medium was removed and the cells washed twice in D-PBS prior to fixation in 10% neutral buffer formalin for 20 min. The fixative was removed and cells exposed to 0.2% Oil Red O for 5 min. Excess stain was removed with isopropanol and cells counterstained with haematoxylin. Images were acquired using the Olympus Ix71 microscope. After visualization, the oil red O was extracted with 100% isopropanol and the absorbance measured at 520nm to determine the total bound oil red O per well.

In the case of osteogenesis, the MSCs were plated in a 6-well plate at density of 2 x 10^4 cells/cm^2 and treated with osteogenic medium (Dulbecco's modified Eagle's medium (DMEM) low glucose, 10% FBS, 1% P/S, 0.1µM dexamethasone, 50µM ascorbic acid 2-phosphate and 10mM β-glycerophosphate) for 14-17 days. The osteogenic medium was replaced every 3 days and harvested after 14 days culture. Following careful washing with PBS, the cells were scraped and transferred into 1ml of 0.5M HCl and placed in an orbital shaker at 4°C overnight. After centrifugation, the debris was removed and the calcium concentration was determined using a Stanbio Calcium (CPC) LiquiColor® Test Kit (Lonza, UK). The calcium solution in the kit was used to generate a standard curve from which it was possible to determine the calcium concentration from the absorbance measured at 550nm on a microplate reader (FLX800, Biotek Instruments Inc.). Calcium deposition was also assessed visually using Alizarin Red S: medium was removed and cells fixed in ice cold 95% methanol for 10 min after washing twice with D-PBS. After rinsing in distilled water, the plate was stained with a 2% Alizarin Red S solution for 5 min. Calcium deposits were visualized and imaged using light microscopy (Olympus IX71 microscope).

For chondrogenesis, 2.5 x 10^5 rabbit MSCs were cultured in complete chondrogenic medium (CCM) consisting of HG-DMEM supplemented with 100nM dexamethasone, 50µg/ml ascorbic acid, 40µg/ml L-Proline, 6.25µg/ml selenous acid, 5.33µg/ml linoleic acid, 1.25mg/ml bovine serum albumin, 0.11mg/ml sodium pyruvate, 1% P/S and 10ng/ml transforming growth factor

(TGF)-β3) with medium changed every 2 days. After 21 days in pellet culture, the cell culture medium was removed and the pellets were washed twice with D-PBS, fixed with 10% neutral buffer formalin for 20 min and washed again with D-PBS. The fixed pellets were dehydrated in a series of alcohols from 50% to 100% and infiltrated with paraffin (Leica EG/550H wax embedder). Thereafter, the samples were de-paraffinized using xylene and rehydrated in alcohol. Sections were stained with 1% toluidine blue for 5 min at 60°C. Images were acquired using a digital camera and Olympus BX51 Upright Fluorescent Microscope with Improvision Optigrid System linked to camera microscope."

16) Discussion, line 1: Add "et al." after "Lee". Applies to all cases with 3+ authors (e.g., Chou, etc.), please revised document thoroughly and carefully in this regard.
Action: et al. has been added to all cases with 3+ authors throughout the manuscript.

17) Discussion: If mechanical testing was done in dry conditions at room temperature, this needs to be mentioned as a caveat when comparing to cartilage moduli range. Material moduli are not expected to be the same if tested under hydrated conditions at 37 degC.
Action: Extra information has been added to the text to account for the fact that the samples were tested dry at room temperature.
Page 19: "However, it must be noted that compression testing of the macroporous PLCL scaffolds was performed on dry samples at room temperature and that future studies will be conducted to examine the mechanical properties of constructs stored in simulated physiological solutions at 37°C to allow better comparison with the mechanical properties of cartilage in addition to examining the changes that occur over time."

18) Discussion: Make sure to consistently refer to your results in the past tense.
Action: The discussion was read carefully and references to results were checked to ensure they were discussed the past tense.

19) Remove the conclusion that "Although the rabbit MSC-seeded scaffold stained positive for toluidine blue, the cells observed are smaller suggesting that they are the rabbit MSCs rather than endogenous cells from the joint such as those observed in the cell-free construct."
Action: This sentence was removed.

20) FTIR could be a supplementary figure instead.
FTIR spectra were added as a supplementary figure.

21) Immunohistochemistry: Methods indicate DAB (brown) was used, but staining appears to be more purple in nature. Please correct methods or clarify. Figure legend is advised to include a reminder of the color that indicates a positive stain.
Action: The figure legend has been changed to show the methods used.

Figure 5B “Collagen type II staining is positive in the adjacent tissue of the empty defect and in between and adjacent to the struts in the cell-free construct (brown DAB positive stain together with pink-eosin counterstain). The brown colour as evidence of collagen type II is less apparent in and around the struts of the cell-seeded constructs”

22) Figures

a. **Remove scale bar lengths from the figures themselves and indicate from the figure legend alone.**

The scale bar lengths have been removed from the figures and are indicated in the text.

b. **Fig. 1B: Rephrase “Mean values for compressive strength at 50% strain of 8.5MPa…”, this does not make sense.**

Action: The figure legend was changed. “Bar graph showing compressive stress at 50% strain, compressive modulus, and modulus of resilience. Values indicate means ± S.E.M.”

c. Figure caption 1B: Indicate values are means and S.E.M.

Action: Figure caption indicate values are means and S.E.M. “Bar graph showing compressive stress at 50% strain, compressive modulus, and modulus of resilience. Values indicate means ± S.E.M.”

d. **Figure numbering gets confusing, can figures be split up to avoid the “i, ii, iii” nomenclature?**

Figure 2A has been moved to the supplementary figures. Figures 3 showing data on rabbit MSC isolation and characterisation has been split in to two figures, with Figure 3 now showing information on MSC growth characteristics and morphology and Figure 4 showing information on tri-lineage differentiation. As a result of this change, Figure 5 became Figure 6. Figure 6 was split into two sections, with Figure 6 showing toluidine blue staining and Figure 7 showing collagen type II and collagen type I staining.

e. Figure 2Bvi: replace p = 0.0426 with p < 0.05. For the other values of p = 0.0005 and 0.01, are those exact values, or would an inequality be more appropriate?

Action: p=0.0426 was replaced with p<0.05. The other values where exact values were used were changed to inequality to keep the format consistent.

f. Increase font size in the legend in Fig. 3C

The font size was increased in Figure 3

g. Figure 3: Indicate the stains written in the actual figure itself. Much easier for readers to follow that way.

Action: The stains have been written on the figures to make them easier to understand.

h. Do the magnifications in Fig. 4 include eyepiece magnification?
No, the magnifications do not include the eye magnification. The figure legends have been altered to take this into account.

i. **Histology resolution inadequate. Need to improve resolution for figures, especially so the reader can zoom in on cells.**
Action: The images were pasted in to word as pictures so the resolution was lost. High quality images have been included in the revised version.

NOTE: Point 15 Methods for tri-lineage differentiation of rabbit MSCs. These methods were optimized by Dr. Khalid Merghani Salid Mohamet, and as a result we would like to include him as an author.

Evaluation of the Early *In vivo* Response of a Functionally Graded Macroporous Scaffold in an Osteochondral Defect in a Rabbit Model

Valerie Barron[1¥], *Martin Neary*[1], *Khalid Merghani Salid Mohamed*[1], *Sharon Ansboro*[1], *Georgina Shaw*[1], *Grace O'Malley*[1], *Niall Rooney*[2], *Frank Barry*[1], *Mary Murphy*[1*]

[1]Regenerative Medicine Institute (REMEDI), Biosciences, National University of Ireland Galway, Galway, Ireland

[2]Proxy Biomedical Ltd., Coilleach, Spiddal, Co. Galway, Ireland

***Corresponding author:** Mary.Murphy@nuigalway.ie

[¥]current address: Materials Research Institute, Athlone Institute of Technology, Dublin Road, Co. Westmeath, Ireland.

Abstract

Cartilage tissue engineering is a multifactorial problem requiring a wide range of material property requirements from provision of biological cues to facilitation of mechanical support in load-bearing diarthrodial joints. ~~As a consequence~~ The study aim was to design, fabricate and characterize a template to promote endogenous cell recruitment for enhanced cartilage repair~~, the main aim of this study was to design, fabricate and characterize a biomimetic template with compressive properties similar to native cartilage and a chondromimetic environment to promote endogenous cell recruitment for enhanced repair~~. ~~Using laser micro-machining technology in combination with thermal crimping methods, a~~A polylactic acid poly-ε-caprolactone (PLCL) support structure was fabricated using laser micromachining technology and thermal crimping to create ~~with~~ a functionally-graded open pore network scaffold with~~,~~ a compressive modulus of 10MPa and a ~~compressive strength~~compressive stress at 50% strain of 8.5MPa. In parallel, rabbit mesenchymal stem cells (MSC) were isolated and their growth characteristics, morphology and multipotency confirmed. ~~Post s~~Sterilization~~, there was no change to the~~ had no effect on construct chemical structure ~~of the construct~~ and cellular compatibility was confirmed. After four weeks implantation in an ~~subchondral~~osteochondral defect in a rabbit model to assess biocompatibility, there was no evidence of inflammation or giant cells. Moreover, acellular constructs performed better than cell-seeded constructs with endogenous progenitor cells homing through ~~the~~ microtunnels, differentiating to form neo-cartilage and strengthening integration with native tissue. These results suggest, albeit at an early stage of repair, that by modulating the architecture of a macroporous scaffold, pre-seeding with MSCs is not necessary for hyaline cartilage repair.

Introduction

Once damaged by osteoarthritis or trauma, self-repair/regeneration of articular cartilage is limited. Current medical treatments include debridement, marrow stimulation using microfracture techniques and osteochondral grafting. Although in the shorter term, these techniques improve mobility and alleviate pain, fibrous cartilage does not possess the optimal biological and mechanical properties to provide a long-term solution.[21] More recently, autologous chondrocyte implantation (ACI), a cell-based therapy, which involves the implantation of expanded autologous chondrocytes under a periosteal patch, has demonstrated improvement in function, reduction in pain and some hyaline cartilage regeneration. However, this technique has not been readily adopted due to cost, technical challenges associated with surgery and post-surgical complications with the periosteal patch.[3] This in turn has led to the development of cell-free membranes such as Chondro-gide® and cartilage treatment options such as the Cartilage Autograft Implantation System (CAIS) and deNovo natural tissue (deNovoNT®).[6] Since its introduction, matrix-induced autologous chondrocyte implantation, or MACI has produced optimistic yet mixed results in clinical trials,[22] leading to the European Medical Agency requesting 5-year follow-up data to allow a better comparison with microfracture over time for marketing authorisation.[5] Nonetheless, it is designed as a periosteal flap replacement to retain autologous chondrocytes at the site of injury rather than providing a biomimetic support structure for endogenous cell recruitment. Development of advanced functional biomaterials to recruit host stem cells to promote regeneration and repair of articular cartilage may represent a biomedical engineering-based alternative to current strategies for repair of articular cartilage defects.

Over the past 20 years, tissue-engineering strategies have been developed for the repair and regeneration of damaged articular cartilage. Early attempts focused on the development of a range of degradable polyester constructs such as polylactic acid (PLA), polyglycolic acid (PGA) and polylactic acid glycolic acid (PLGA) meshes and sponges with design criteria such as pore interconnectivity, porosity and degradation rate investigated for optimal cell viability and neotissue integration.[7,8,11] However, *in vivo* cartilage repair was not optimal and it was suggested that better repair could be achieved by tailoring the mechanical properties of constructs to mimic the native mechanical properties of articular cartilage.[27] In terms of identifying the exact mechanical property requirements for native cartilage, large variations can be observed in the literature due to differences in donor age, tissue isotropy, biochemical composition and state of degeneration. Nonetheless, using computational analysis, it was found that the optimal elastic modulus for a construct for osteochondral repair lies between 1 and 50MPa; above or below these values cartilage formation decreased, while fibrous tissue and bone formation increased.[18] Moreover, it was also revealed that the optimal compressive modulus for functional tissue support was in the region 1-12MPa.[12] Using this approach, Malda *et al.* developed a polyethylene terephthalate/polybutylene terephthalate (PEOT/PBT) polymer with a finely-tuned biochemical composition and dynamic stiffness values matching that of native cartilage.[23] Although the chemical composition had been custom-made for cartilage applications, the architecture of the construct lacked depth-dependent mechanical properties. In an effort to overcome this limitation, Lee *et al.* developed a cell-free polycaprolactone (PCL)-based construct with a functional graded pore architecture with 400μm pores on the top surface through to 200μm pores on the bottom surface that displayed promising cartilage repair *in vivo*.[19] More

recently, Mendoza-Palomares *et al.* developed a smart hybrid system equipped with nanoreservoirs of therapeutic agents, which promoted cartilage repair in an osteochondral defect.[24] These studies present an alternative approach to that of scaffolds seeded with cells to promote hyaline cartilage repair. Not only will waiting periods associated with cell harvesting and expansion for ACI and MACI be reduced but just one surgical intervention will be required.

In parallel, other researchers have begun to investigate the effect of polymer degradation rate on the inflammatory response of medical implants *in vivo*, where it has been shown that biocompatibility is improved in the presence of slowly degrading materials.[13] In particular, the first 28 days in the repair process are critical[9] as undesirable polymer degradation products can provoke an inflammatory response and adversely affect the repair process. We hypothesized that by striking a balance between pore architecture, mechanical properties and degradation rate of the scaffold, enhanced repair could be achieved. Specifically, the main objectives of this study were (1) to fabricate 3D porous constructs with an open tunnel network and mechanical properties similar to those proposed by previous studies[18] and ~~to fabricate 3D constructs with the physical architecture and compressive properties of native tissue~~ (2) to examine inflammation and early chondrogenic response in an defect in a rabbit model.

Materials and Methods

Materials

All materials were purchased from Sigma Aldrich, Dublin, Ireland unless specified.

Scaffold fabrication

Based upon the materials property requirements described above, a 70:30 polylactic acid poly-ε-caprolactone (PLCL) copolymer with an intrinsic viscosity midpoint of 1.5 dl/g (PURASORB PLC7015, Purac Corbion, Amsterdam, The Netherlands) was selected as the material for the construct. Using laser micro-machining technology in combination with thermal crimping a 3D porous substrate with a functionally-graded pore structure was created to mimic the orientation and distribution of cells in native hyaline cartilage.

Physical characterisation of the scaffold

The 3D architecture of the PLCL construct was imaged using micro computed tomography (SCANCO Medical AG Bassersdorf, Switzerland) high resolution scans, with a resolution of 6 microns using 70 kVp, 114 μμA and 8 Watts. In parallel, the open pore tunnel structure was visualized using scanning electron microscopy (SEM) (Hitachi, S4700, UK). In brief, samples were sputter coated with gold and imaged using a 15kV accelerating voltage for analysis of pore size, pore shape and open microtunnel observation. Additionally, to ensure reproducibility and reliability of the fabrication methods, the polymer morphology and molecular weight was examined using differential scanning calorimetry, thermal gravimetric analysis and gel permeation chromatography (See supplementary data).

Mechanical testing

Compression testing was performed on as-fabricated dry samples on a Zwick mechanical testing machine (Zwick, UK) at room temperature using a load cell of

100N and a crosshead speed of 10mm/min according to ASTM-D695-10 (n=5). An initial tare load of 0.2 N was applied to the sample. Stress strain curves were generated from which it was possible to determine the elastic compressive modulus from the slope of the linear region, the compressive ~~strength~~ stress at 50% strain and the resilience from the area under the curve.

Sterilization

After fabrication, the PLCL scaffolds were sterilized by gamma irradiation using a 25kGy dose. To ensure that there was no change in the chemical properties of the scaffolds, the chemical structure was analyzed using Fourier transform infra-red spectroscopy (FTIR-8300, Shimadzu, UK). Spectra were recorded in the wavelength range 4000cm^{-1} to 400cm^{-1} by 2cm^{-1} resolution in 32 scans and in 10 different areas for each specimen (n=6). In addition, cytotoxicity test methods were conducted in accordance with ISO 10993-12 to examine the cell response after sterilization, using human bone-marrow derived MSCs as a cell source, since the ultimate application was for human use. In brief, the MSCs at passage 3 (n=3 technical replicates from one male donor aged 24) were seeded at a density of 2 x 10^4 cells/cm^2 and maintained for 24h at 37°C in a humidified atmosphere and 5% CO_2. In parallel, the constructs were immersed in MSC culture medium [α-minimum essential medium (α-MEM, Gibco, Thermo Fisher, Dublin), 10% fetal bovine serum and 1% penicillin/streptomycin] to create conditioned medium After 24h the PLCL constructs were placed on the cells for direct contact analysis, while the conditioned medium was used in parallel for MSC growth (n=6). An AlamarBlue™ assay (~~Molecular Probes~~Lifescience Technologies, Thermo Fisher, Dublin) was employed to examine MSC metabolic activity after 72h by measuring the absorbance at 550nm and

595nm. Cell number was also assessed using a PicoGreen dsDNA quantification fluorescence assay (~~Molecular Probes~~Lifescience Technologies, Thermo Fisher Dublin) (485nm excitation/535 nm emission) on a plate reader. As a method of control MSC were seeded on tissue culture plastic.

Isolation and characterization of rabbit mesenchymal stem cells

To assess the early repair response *in vivo*, MSC were obtained from the tibia of skeletally mature male (>3kg) ~~white New Zealand rabbits~~New Zealand white rabbits (Charles River, France) (n=6). All procedures including bone marrow harvest were conducted with approval from the National University of Ireland Galway's Animal Care and Research Ethical Committee. A disposable 18-gauge intraosseous infusion needle was used to access the bone marrow compartment in the tibia with radiographic guidance (GE OEC 9800 Plus) under anaesthesia. Bone marrow (5ml) was aspirated into a syringe containing 1ml heparin diluted to 3,000units/ml in saline and transferred to a 50ml sterile tube. Bone marrow aspirates were washed with Dulbecco's phosphate buffered solution (D-PBS) and filtered using a 70µm cell strainer. Mononuclear cells (MNC) were cultured at 37°C in 5% CO_2 and a humidified atmosphere at a density between 100,000 – 115,000 cells/cm^2 in control culture medium (α-MEM. Gibco-UK) containing 10% fetal bovine serum and 1% penicillin/streptomycin (P/S), enriched medium with 2% rabbit serum (R4505, Sigma, Dublin,~~R4505~~). Once confluent, cells were detached using 0.25% trypsin/EDTA for 5 min at 37°C and passaged at a density of 5,500 cells/cm^2. Cell morphology was observed using light microscopy (Olympus IX71 microscope). CFU-F assays were conducted for each marrow with 3 x 10^6 MNCs cultured in 10cm tissue culture dishes

(n=3 for 2 donors) until discrete colonies were observed. Medium was removed and colonies fixed with 90% methanol prior to staining with 2% crystal violet (C0775, Sigma, Dublin). The dishes were imaged using a flatbed scanner (Epson Stylus Sx425W) and the number of colonies quantified using ImageJ analysis. Growth kinetics of the rabbit MSC cultures with or without 2% rabbit serum were evaluated over a 30-day cell culture period by calculating the cumulative population doublings. Thereafter, tri-lineage differentiation was examined using methods previously described.[25] For adipogenesis, confluent cultures were exposed to induction medium (DMEM high glucose (HG-DMEM), 10% FBS (Hyclone, Logan, UT, USA), 1% P/S, 10µg/ml insulin, 1µM dexamethasone, 500µM isobutylmethylxanthine and 200µM indomethacin) for 3 days, followed by 1-3 days in maintenance medium (DMEM high glucose, 10% FBS, 1% P/S and 10µg/ml insulin). The cycle was repeated 3 times with cells left in maintenance medium for 7 days in total prior to harvesting for analysis. At the end of the culture period, medium was removed and the cells washed twice in D-PBS prior to fixation in 10% neutral buffer formalin for 20 min. The fixative was removed and cells exposed to 0.2% Oil Red O for 5 min. Excess stain was removed with isopropanol and cells counterstained with haematoxylin. Images were acquired using the Olympus Ix71 microscope. After visualization, the oil red O was extracted with 100% isopropanol and the absorbance measured at 520nm to determine the total bound oil red O per well.

In the case of osteogenesis, the MSCs were plated in a 6-well plate at density of 2 x 10^4 cells/cm^2 and treated with osteogenic medium (Dulbecco's modified Eagle's medium (DMEM) low glucose, 10% FBS, 1% P/S, 0.1µM dexamethasone, 50µM ascorbic acid 2-phosphate and 10mM β-glycerophosphate) for 14-17 days. The

osteogenic medium was replaced every 3 days and harvested after 14 days culture. Following careful washing with PBS, the cells were scraped and transferred into 1ml of 0.5M HCl and placed in an orbital shaker at 4°C overnight. After centrifugation, the debris was removed and the calcium concentration was determined using a Stanbio Calcium (CPC) LiquiColor® Test Kit (Lonza, UK). The calcium solution in the kit was used to generate a standard curve from which it was possible to determine the calcium concentration from the absorbance measured at 550nm on a microplate reader (FLX800, Biotek Instruments Inc.). Calcium deposition was also assessed visually using Alizarin Red S: medium was removed and cells fixed in ice cold 95% methanol for 10 min after washing twice with D-PBS. After rinsing in distilled water, the plate was stained with a 2% Alizarin Red S solution for 5 min. Calcium deposits were visualised and imaged using light microscopy (Olympus IX71 microscope).

For chondrogenesis, 2.5 x 10^5 rabbit MSCs were cultured in complete chondrogenic medium (CCM) consisting of G-DMEM supplemented with 100nM dexamethasone, 50µg/ml ascorbic acid, 40µg/ml L-Proline, 6.25µg/ml selenous acid, 5.33µg/ml linoleic acid, 1.25mg/ml bovine serum albumin, 0.11mg/ml sodium pyruvate, 1% P/S and 10ng/ml transforming growth factor (TGF)-β3) with medium changed every 2 days. After 21 days in pellet culture, the cell culture medium was removed and the pellets were washed twice with D-PBS, fixed with 10% neutral buffer formalin for 20 min and washed again with D-PBS. The fixed pellets were dehydrated in a series of alcohols from 50% to 100% and infiltrated with paraffin (Leica EG/550H wax embedder). Thereafter, the samples were de-paraffinized using xylene and rehydrated in alcohol. Sections were stained with 1% toluidine blue for 5 min at

60°C. Images were acquired using a digital camera and Olympus BX51 Upright Fluorescent Microscope with Improvision Optigrid System linked to camera microscope.

Animal surgery

Nine skeletally mature male ~~White New Zealand rabbits~~New Zealand white rabbits, weighing more than 3kg were used in this study to evaluate biocompatibility and early repair. Both knees in each rabbit underwent surgery under sterile conditions. In total 18 knees were randomly assigned into three groups, including empty defect (n=5 knees, with 6 technical replicates - one rabbit received two empty defects, one in the left knee and one in the right as a result of the randomization), cell-free constructs (n=5 knees, with 6 technical replicates - one rabbit received two cell-free constructs, one in the left knee and one in the right as a result of the randomization) and MSC-seeded constructs (n=6 knees).~~In total 18 knees were randomly assigned into three groups, including empty defect (n=6 knees), cell-free constructs (n=6 knees) and MSC-seeded constructs (n=6 knees).~~ Briefly, the rabbits were anaesthetized using a weight-adjusted dose of ketamine (35mg/kg) and xylazine (10mg/kg). The operative leg was secured in a retort stand and access to the knee joint achieved via an anterior midline skin incision, followed by a medial para-patellar joint capsule incision. The patella was dislocated laterally to provide increased exposure of the medial femoral condyle. To facilitate testing of these constructs, which were custom designed for human chondral defects with dimensions of 3mm in diameter and 1mm in height, a 1mm shallow osteochondral ~~subchondral~~ defect was created on the medial femoral condyle using a drill with a previously sterilized 2.8mm drill bit covered with a sterile depth stop. The walls of the defect were finished with a

dental curette, and the constructs were press-fit into place. The cell-seeded constructs were cultured in serum-free cell culture medium (HG-DMEM supplemented with 100nM dexamethasone, 50µg/ml ascorbic acid, 40µg/ml L-Proline, 6.25µg/ml selenious acid, 5.33µg/ml linoleic acid, 1.25mg/ml bovine serum albumin, 0.11mg/ml sodium pyruvate, 1% penicillin/streptomycin) for 24h prior to surgery, using a cell seeding density of $1.2X10^6$ syngeneic rabbit MSC (passage one) per construct as previously described.[17]

Histological staining for inflammation

After 4 weeks, the rabbits were sacrificed and post examination of gross surface morphology the femoral condyles were removed and fixed in 10% neutral buffered formalin for 10 days as previously described.[29] Following fixation, samples were decalcified in Surgipath® for 2-3 weeks, with solution changes every 3 days. Decalcification was deemed to be complete following 2 consecutive negative tests for residual calcium using equal volumes of 5% ammonium oxalate and 5% ammonium hydroxide and decalcifying solution. After processing and paraffin embedding, histological sections (5µm) were dewaxed at 65°C, immersed in histoclear and rehydrated in a series of alcohols 100%, 95% and 70% prior to staining with H&E for assessment of an inflammatory response. Briefly, sections were exposed to Harris hematoxylin ~~(Sigma)~~ for 7 min, blued in Scott's tap water substitute ~~(Sigma)~~ for 2 min and counterstained with eosin Y ~~(Sigma)~~ for 7 min.

Staining for early chondrogenesis and repair

Sections were stained for evidence of early chondrogenesis using toluidine blue (TB). Positive collagen type II immunostaining was used to assess the presence of hyaline cartilage and collagen type I used to assess fibrous cartilage. For collagen type I and II immunostaining, an endogenous hydroxide quench was performed with 0.3% hydrogen peroxide (H_2O_2) in methanol after rehydration. Thereafter, antigen retrieval was performed using pepsin (DAKO, S3002 4% in 0.2N HCl, Agilent Technologies, Dublin) for 30 min, followed by blocking with 5% rabbit serum in tris-buffered saline (TBS 0.05M tris, 0.15M NaCl, pH 7.6) for collagen type I and 10% goat serum (KPL 71-00-27, Insight Biotechnology, Middlesex) in TBS for collagen type II. Sections were incubated overnight at 4°C with goat polyclonal anti-type I collagen antibody (1:100, S1301-01, Southern Biotech, Birmingham, AL, USA, ~~S1301-01~~) and with mouse monoclonal anti-rabbit type II collagen antibody (1:50; AF5710, Acris, Herford, Germany ~~AF5710~~). Sections were then incubated with biotinylated secondary antibodies against rabbit anti-goat (H+L) (1:1000; 305-065-003 Jackson ImmunoResearch, Newmarket) ~~305-065-003)~~ for collagen type I or goat anti-mouse (H+L) (1:1000; KPL 71-00-29, Insight Biotechnology, Middlesex) for collagen type II followed by peroxidase-conjugated streptavidin (KPL 71-00-38) at room temperature for 30 min each and stained for visualization with 3,3' diaminobenzidine (DAB) (Abcam, substrate kit, ab94665, Cambridge, UK). Sections were counterstained with Harris hematoxylin ~~(Sigma)~~ for 10 sec and eosin-phloxine B ~~(Sigma)~~ for 1 min. After staining, all sections were dehydrated in a series of alcohols (70%, 95% and 100%), cleared with histoclear and mounted using histomount for imaging using the Olympus BX51 Upright Fluorescent Microscope.

Statistical Analysis

Compressive property data are expressed as means ± standard error of the mean (SEM). Colony formation and cytotoxicity studies were analyzed using a student's t test with $p \geq 0.05$ considered not significant (ns). All data was analysed using GraphPad Prism version 6.

Results

3D construct with open pore microtunnel structure

A biomimetic architecture was created by a combination of laser machining and precise offsetting of the various layers resulted in an open pore structure, with microtunnels visible from the top surface through to the bottom (Fig. 1 and supplementary video). Using SEM (Fig. 1), it can be seen that the pore size increases from 180µm in diameter at the top (Fig. 1Ai) to 200µm X 600µm at the bottom surface of the construct (Fig. 1Aii) creating an open tunnel through the structure (Fig. 1Aiii).

Compressive properties of the 3D scaffold

The stress strain curves generated from the compression test are shown in Fig. 1B~~2B~~i, where it can be seen that a similar curve was generated for each sample and that the PLCL constructs had a mean compressive modulus of 10 ± 1.41 MPa, a mean ~~compressive strength~~compressive stress at 50% strain of 8.5 ± 1.35 MPa and a mean recoverable elastic energy per unit volume that can be stored in the polymer or modulus of resilience value of 1.5 ± 0.12 MPa (Fig. 1Bii)~~.~~

Sterilization

Sterilization by gamma irradiation did not affect the chemical structure of the PLCL copolymer with no difference observed in the characteristic PLCL peaks at 1050-1180cm^{-1} for C-O-C, 1750cm^{-1} for C=O and 3000cm^{-1} for CH groups using FTIR spectroscopy (see supplementary figure~~Fig. 2A~~). The metabolic activity of human MSCs was examined for cells cultured in direct contact with the scaffold and using conditioned medium (Fig. 2~~B~~). As shown in Fig. 2~~B~~i, Fig. 2~~B~~ii and Fig. 2~~B~~iii, there was no statistically significant difference ~~statistical difference~~ observed in metabolic activity, cell number or normalized metabolic activity per cell number for cells grown in the presence of the PLCL construct. In contrast, a ~~statistical~~ significant difference was observed in metabolic activity (Fig. 2~~B~~iv), cell number (Fig. 2~~B~~v) and normalized metabolic activity per cell number (Fig. 2~~B~~vi) for cells grown in conditioned medium, where a 19% increase in metabolic activity, a 32% increase in cell number and a 26% decrease in normalized metabolic activity per cell number was observed.

MSC growth characteristics

As shown by crystal violet staining in Fig. 3A, rabbit MSCs did not form colonies efficiently in the absence of 2% rabbit serum. Quantification of CFU-F data indicated double the number of colonies in supplemented cultures, with average values of 40 recorded without and values of over 80 recorded in the presence of 2% rabbit serum (Fig. 3B). In terms of cumulative population doublings, the cells did not proliferate in the absence of rabbit serum after P0 (Fig. 3C). Moreover, the cells did not maintain their characteristic MSC morphology and were much larger and flatter in the absence of rabbit serum (Fig. 3Di, black arrows).

Tri-lineage differentiation of rabbit MSCs

The differentiation potential of the rabbit MSCs was examined with and without 2% rabbit serum (Fig. 4), with oil red O staining confirming the presence of adipocytes (Fig. 4i, ii), calcium deposition providing evidence of osteogenesis (Fig. 4iii, iv) and GAG accumulation as illustrated by positive staining for toluidine blue providing evidence of chondrogenesis (Fig. 4vi). Differentiation was observed in all cases in the presence of 2% rabbit serum, with oil red O (Fig. 34i,ii) and calcium deposition (Fig. ~~3E~~ 4iii, iv) highlighted with the black arrows, where it can be seen that both adipogenesis and osteogenesis is much more evident in the presence of the serum. Moreover, in the absence of rabbit serum, the rabbit MSCs were unable to condense and form a pellet, while in the presence of 2% rabbit serum chondrogenesis was observed in the pellet shown in Fig. ~~3E~~4(vi).

Inflammation and biocompatibility

Hematoxylin and eosin (H&E) staining was used to evaluate whether there was an adverse effect to the surrounding tissue after 4 weeks implantation. As expected, tissue fill was observed for the empty defect, highlighted by the box with dotted lines. However, there was no evidence of inflammation or giant cells in the cell-free construct or the cell-seeded construct in the representative images shown in Fig. ~~4~~5.

Assessment of chondrogenesis and early repair

Evidence of chondrogenesis, neo-tissue formation and integration was examined using toluidine blue staining. In the montage of images from all defects shown in the supplemental figures, fibrous tissue fill can be seen in three of the empty defects,

with the other three defects remaining empty. In comparison, four of the defects containing cell-free constructs revealed evidence of cartilaginous neotissue formation in and around the struts of the scaffold, with two defects appearing to remain empty. A similar trend was observed for the cell-seeded scaffolds, with only two defects appearing empty. As shown in Figure 6, lateral integration with native cartilage in the empty defect was observed to be incomplete as highlighted by the black arrow. In contrast, it can be seen that there was evidence of integration between the host tissue and the cell-free construct. At lower magnification, the scaffold appeared to be integrated at the bottom and at both sides of the defect and lateral integration with host tissue is emphasized in the 10x representative image. Of relevance is the appearance of round, toluidine blue-positively stained cells with a chondrocytic morphology seen at 20x, suggesting that the underlying bone marrow diffused in and around the scaffold struts, resulting in early chondrogenesis. With respect to the cell-seeded construct, the sections also stained positive for toluidine blue, but there was less evidence of neo-tissue organization or integration as indicated by the black arrow.~~Evidence of chondrogenesis, neo-tissue formation and integration was examined using toluidine blue staining as shown by representative images in Fig. 5A. For the empty defect (fibrocartilage control), tissue fill was observed at all magnifications, but at higher magnification (10x), lateral integration with native cartilage was observed to be incomplete as highlighted by the black arrow. In contrast, it can be seen that there was evidence of integration between the host tissue and the cell-free construct. At lower magnification, the scaffold appeared to be integrated at the bottom and at both sides of the defect and lateral integration with host tissue is emphasized in the 10x representative image. Of relevance is the~~

~~appearance of round, toluidine blue-positively stained cells with a chondrocytic~~

Regarding hyaline cartilage repair, collagen type II staining was observed in and around the struts of the cell-free construct; while there was much less evidence of collagen type II in the rabbit MSC-seeded scaffold and no collagen type II in the empty defect (Fig. ~~5B~~7). However, there was evidence of collagen type I staining in all three defects. On closer examination of the cell-free construct (20x), the immature chondrocytes visible around the struts did not stain positive for collagen type I (Fig. ~~5B~~7).

Discussion

In a recent study by Lee *et al.*,[19] it was suggested that a functionally-graded pore architecture promoted endogenous cell recruitment and provided a superior support structure for cartilage repair. To achieve this specific functionality, a support structured was designed and fabricated to mimic both the structure and mechanical properties of native articular cartilage repair. Fig. 1A illustrate~~d~~ds the generation of a biomimetic pore structure, with an open tunnel system, created by the custom-designed layer structure. In addition to creating an open functionally-graded pore template for cells that complements the work of Chou *et al.*[4] and Lee *et al.*,[19] the compressive modulus values were orders of magnitude higher (10 MPa) than previous composite constructs[27] (0.005-0.10 MPa) and represent a step towards mechanical property values proposed for hyaline cartilage regeneration in the region 1-12MPa.[12] However, it must be noted that compression testing of the macroporous PLCL scaffolds was performed on dry samples at room temperature and that future studies will be conducted to examine the mechanical properties of constructs stored

in simulated physiological solutions at 37°C to allow better comparison with the mechanical properties of cartilage in addition to examining the changes that occur over time.

Regarding sterilization, there were no changes observed in the chemical structure of the polymer post gamma irradiation. In terms of *in vitro* cell response, cells exposed to conditioned medium were healthy and proliferated well with significantly increased metabolic activity and cell number compared to control cells. When metabolic activity was normalised to cell number, the data did suggest a minimal negative effect of the conditioned medium that did not translate to a biological effect, as the cells were metabolically active and the chemical structure of the polymer was unaltered. This is in line with Wang *et al.*, where low concentrations of polymer eluates in conditioned medium were shown to increase cell numbers without adversely affecting cell viability or biocompatibility[30] of ultra-high molecular weight polyethylene for hip joint applications.

Previous studies ~~have~~ successfully employed bone marrow-derived MSCs for cartilage repair applications. In a recent publication, it was revealed that rabbit MSCs bec~~a~~ame senescent when expanded in culture.[24] In an effort to overcome this limitation, rabbit cells were cultured in cell culture medium containing 2% rabbit serum. To ensure the MSCs retained their plasticity, tri-lineage differentiation assays were performed. As shown, the cells retained their MSC characteristics, did not lose their tri-lineage potential as described by Ahmadbeigi *et al.*,[1] when cultured in the presence of 2% rabbit serum. These assays confirmed the phenotype of the optimized rabbit MSC preparations *in vitro* and validated their use *in vivo*.

In relation to limitations of the animal study, the number of replicates is noted. Due to the randomization, one rabbit received two empty defects, one in the left knee and one in the right and another rabbit received two cell-free constructs, one in the left knee and one in the right. As shown in montage of images in the supplemental figures, there was no trend for repair in the rabbit that received an empty defect in both knees, with one knee remaining empty and the other showing evidence of tissue fill, albeit fibrous tissue formation. With respect to the rabbit that received two cell-free constructs, there is evidence of neotissue formation and chondrogenesis in both knees. The number of specimens analyzed was sufficient to compare biocompatibility and early repair, but larger numbers of rabbits, with different test groups in different knees are required for the 12-week cartilage repair proof of principle studies recommended by the International Society for Cartilage Repair (ICRS).[10]

Regarding inflammation, the PLCL scaffold was biocompatible with no evidence of inflammation or giant cells in or around the struts of the template after 4 weeks implantation, which agrees well with previous studies by Jung *et al.*,[15,16] where PLCL was also shown not to evoke an adverse inflammatory response *in vivo*. On first observation, it appeared that the tissue repair in the empty defect was better than that of the scaffolds. However, on closer examination, it was seen that the repair tissue was fibrous primarily, as evidenced by the presence of collagen type I staining and the absence of collagen type II staining. Moreover, there was evidence of chondrocyte clustering and hypo- and hyper-cellularity in the repair and native tissues adjacent to the empty defect, which compared well with previous findings where fibrous tissue formation was observed in empty defects and is perhaps why empty defects, are accepted as a negative control ~~defects.~~.[2,10] Of more interest was

the fact the functionally-graded pore structure appeared to go one step forward compared to Jung[15,16] and enhanced endogenous cell recruitment, integration and neotissue formation, with immature chondrocytes and collagen type II staining visible throughout and under the cell-free PLCL construct. This correlates well with other studies, where cartilage repair was attributed to cell homing, engraftment and repair due to pore architecture of the construct used.[4,9,19] Despite that collagen type I staining was observed in all defects in the present study, chondrocytes adjacent to the cell-free construct did not stain positive. Although, collagen type I is associated with fibrocartilage repair, spatial and temporal patterns of collagen type I expression have been observed during cartilage development,[26] at early time points during *in vitro* chondrogenesis of MSC[14] and after ACI in humans.[20] Therefore, longer time points are required to determine whether the collagen I staining observed in this study occurreds as a result of early hyaline cartilage or fibrocartilage development. The addition of the MSC to the PLCL construct did not appear to enhance hyaline cartilage formation. The immature chondrocytes visible in the cell-free construct weare not as evident and lateral integration with native tissue did oes not appear to be as good as the cell-free construct, which correlatedds well with the previous studies where the presence of MSCs was believed to impair cell homing and better cartilage repair.[9,28] Since the materials properties and architecture of the functionally-graded scaffold are promising, these results suggest that instead of altering the surface chemistry, mechanical properties or pore architecture as a next step, proof of principle studies such as that recommended by the ICRS with larger numbers and longer time points should be conducted as they would provide very valuable information on the repair potential.

Acknowledgements

The authors would like to acknowledge the help of Ms. Teresa Jungwirth, Regenerative Medicine Institute, NUI Galway and Dr. Declan Devine, Athlone Institute of Technology for his help with differentiatal scanning calorimetry. The authors acknowledge the facilities and technical assistance of the Dr. Cathal O'Flaharta at the NCBES Preclinical Facility Core, National University of Ireland Galway. The research leading to these results has received funding from the European Union's 7th Framework Programme under grant agreement no. HEALTH-2007-B-223298 (PurStem), Science Foundation Ireland (grant number 09/SRC/B1794), Wellcome Trust Biomedical Vacation Scholarships grant number WTD004448 and the Irish Government's Programme for Research in Third Level Institutions, Cycles 4 and 5, National Development Plan 2007-2013.

Competing interest

All authors report no conflict of interest for this work.

References

1. Ahmadbeigi, N., A. Shafiee, E. Seyedjafari, Y. Gheisari, M. Vassei, S. Amanpour, S. Amini, I. Bagherizadeh, and M. Soleimani. Early spontaneous immortalization and loss of plasticity of rabbit bone marrow mesenchymal stem cells. *Cell Prolif.* 44:67–74, 2011.
2. Barron, V., K. Merghani, G. Shaw, C. M. Coleman, J. S. Hayes, S. Ansboro, A. Manian, G. O'Malley, E. Connolly, A. Nandakumar, C. A. van Blitterswijk, P. Habibovic, L. Moroni, F. Shannon, J. M. Murphy, and F. Barry. Evaluation of Cartilage Repair by Mesenchymal Stem Cells Seeded on a PEOT/PBT Scaffold in an Osteochondral Defect. *Ann. Biomed. Eng.* 43:2069–2082, 2015.

3. Brittberg, M. Cell carriers as the next generation of cell therapy for cartilage repair: a review of the matrix-induced autologous chondrocyte implantation procedure. *Am. J. Sports Med.* 38:1259–1271, 2010.
4. Chou, C.-L., A. L. Rivera, T. Sakai, A. I. Caplan, V. M. Goldberg, J. F. Welter, and H. Baskaran. Micrometer Scale Guidance of Mesenchymal Stem Cells to Form Structurally Oriented Cartilage Extracellular Matrix. *Tissue Eng. Part A* , 2012.doi:10.1089/ten.TEA.2012.0177
5. European Medicines Agency. MACI: EPAR Summary for the public. 2014.
6. Farr, J., B. J. Cole, S. Sherman, and V. Karas. Particulated articular cartilage: CAIS and DeNovo NT. *J. Knee Surg.* 25:23–29, 2012.
7. Freed, L. E., I. Martin, and G. Vunjak-Novakovic. Frontiers in tissue engineering. In vitro modulation of chondrogenesis. *Clin. Orthop.* S46–58, 1999.
8. Guilak, F., D. L. Butler, S. A. Goldstein, and D. Mooney. Functional Tissue Engineering. Springer, 2004, 452 pp.
9. Hababovic, P. Predictive Value of In Vitro and In Vivo Assays. In: Tissue Engineering, edited by J. P. Fisher. Springer, 2006.
10. Hurtig, M. B., M. D. Buschmann, L. A. Fortier, C. D. Hoemann, E. B. Hunziker, J. S. Jurvelin, P. Mainil-Varlet, C. W. McIlwraith, R. L. Sah, and R. A. Whiteside. Preclinical Studies for Cartilage Repair Recommendations from the International Cartilage Repair Society. *Cartilage* 2:137–152, 2011.
11. Hutmacher, D. W., K. W. Ng, C. Kaps, M. Sittinger, and S. Kläring. Elastic cartilage engineering using novel scaffold architectures in combination with a biomimetic cell carrier. *Biomaterials* 24:4445–4458, 2003.
12. Jansen, E. J. P., J. Pieper, M. J. J. Gijbels, N. A. Guldemond, J. Riesle, L. W. Van Rhijn, S. K. Bulstra, and R. Kuijer. PEOT/PBT based scaffolds with low

mechanical properties improve cartilage repair tissue formation in osteochondral defects. *J. Biomed. Mater. Res. A* 89:444–452, 2009.

13. Jiang, W.-W., S.-H. Su, R. C. Eberhart, and L. Tang. Phagocyte responses to degradable polymers. *J. Biomed. Mater. Res. A* 82:492–497, 2007.
14. Johnstone, B., T. M. Hering, A. I. Caplan, V. M. Goldberg, and J. U. Yoo. In vitro chondrogenesis of bone marrow-derived mesenchymal progenitor cells. *Exp. Cell Res.* 238:265–272, 1998.
15. Jung, Y., S. H. Kim, S.-H. Kim, Y. H. Kim, J. Xie, T. Matsuda, and B. G. Min. Cartilaginous tissue formation using a mechano-active scaffold and dynamic compressive stimulation. *J. Biomater. Sci. Polym. Ed.* 19:61–74, 2008.
16. Jung, Y., M. S. Park, J. W. Lee, Y. H. Kim, S.-H. Kim, and S. H. Kim. Cartilage regeneration with highly-elastic three-dimensional scaffolds prepared from biodegradable poly(L-lactide-co-epsilon-caprolactone). *Biomaterials* 29:4630–4636, 2008.
17. Kavalkovich, K. W., R. E. Boynton, J. M. Murphy, and F. Barry. Chondrogenic differentiation of human mesenchymal stem cells within an alginate layer culture system. *In Vitro Cell. Dev. Biol. Anim.* 38:457–466, 2002.
18. Kelly, D. J., and P. J. Prendergast. Prediction of the optimal mechanical properties for a scaffold used in osteochondral defect repair. *Tissue Eng.* 12:2509–2519, 2006.
19. Lee, C. H., J. L. Cook, A. Mendelson, E. K. Moioli, H. Yao, and J. J. Mao. Regeneration of the articular surface of the rabbit synovial joint by cell homing: a proof of concept study. *Lancet* 376:440–448, 2010.
20. Løken, S., T. C. Ludvigsen, T. Høysveen, I. Holm, L. Engebretsen, and F. P. Reinholt. Autologous chondrocyte implantation to repair knee cartilage injury:

ultrastructural evaluation at 2 years and long-term follow-up including muscle strength measurements. *Knee Surg. Sports Traumatol. Arthrosc. Off. J. ESSKA* 17:1278–1288, 2009.

21. Longo, U. G., S. Petrillo, E. Franceschetti, A. Berton, N. Maffulli, and V. Denaro. Stem cells and gene therapy for cartilage repair. *Stem Cells Int.* 2012:168385, 2012.
22. Makris, E. A., A. H. Gomoll, K. N. Malizos, J. C. Hu, and K. A. Athanasiou. Repair and tissue engineering techniques for articular cartilage. *Nat. Rev. Rheumatol.* 11:21–34, 2015.
23. Malda, J., T. B. F. Woodfield, F. van der Vloodt, C. Wilson, D. E. Martens, J. Tramper, C. A. van Blitterswijk, and J. Riesle. The effect of PEGT/PBT scaffold architecture on the composition of tissue engineered cartilage. *Biomaterials* 26:63–72, 2005.
24. Mendoza-Palomares, C., A. Ferrand, S. Facca, F. Fioretti, G. Ladam, S. Kuchler-Bopp, T. Regnier, D. Mainard, and N. Benkirane-Jessel. Smart Hybrid Materials Equipped by Nanoreservoirs of Therapeutics. *ACS Nano* 6:483–490, 2012.
25. Mooney, E., P. Dockery, U. Greiser, M. Murphy, and V. Barron. Carbon nanotubes and mesenchymal stem cells: biocompatibility, proliferation and differentiation. *Nano Lett.* 8:2137–2143, 2008.
26. Morrison, E. H., M. W. Ferguson, M. T. Bayliss, and C. W. Archer. The development of articular cartilage: I. The spatial and temporal patterns of collagen types. *J. Anat.* 189:9–22, 1996.
27. Moutos, F. T., L. E. Freed, and F. Guilak. A biomimetic three-dimensional woven composite scaffold for functional tissue engineering of cartilage. *Nat. Mater.* 6:162–167, 2007.

28. Ostrander, R. V., R. S. Goomer, W. L. Tontz, M. Khatod, F. L. Harwood, T. M. Maris, and D. Amiel. Donor cell fate in tissue engineering for articular cartilage repair. *Clin. Orthop.* 228–237, 2001.

29. Ponticiello, M. S., R. M. Schinagl, S. Kadiyala, and F. P. Barry. Gelatin-based resorbable sponge as a carrier matrix for human mesenchymal stem cells in cartilage regeneration therapy. *J. Biomed. Mater. Res.* 52:246–255, 2000.

30. Wang, K. Y., J. G. Horne, P. A. Devane, T. Wilson, and J. H. Miller. Chemical eluates from ultra-high molecular weight polyethylene and fibroblast proliferation. *J. Orthop. Surg. Hong Kong* 9:25–33, 2001.

Figure Captions

Figure 1 (A) Scanning electron microscopy image showing the top surface of the construct with circular pores, 180μm in diameter, (ii) the bottom surface with elliptical pores of dimensions of 200μm x 600μm and (iii) a cross section of the construct with pore size gradient increasing from the top to the bottom with a microtunnel through the construct highlighted in yellow. **(B)** Mechanical properties of the PLCL construct with (i) Stress strain curves generated for PLCL constructs in compression (n=5), (ii) ~~Mean values~~Bar graph showing ~~for compressive strength~~compressive stress at 50% strain~~ of 8.5MPa~~, compressive modulus, ~~of 10MPa~~ and ~~a resilience of 1.5MPa.~~ modulus of resilience. Values indicate means ± S.E.M.

Figure 2 ~~**(A)** FTIR spectroscopy spectra showing that sterilization using gamma irradiation has no effect on the chemical properties of the copolymer, with characteristic PLCL peaks between 1050-1180cm^{-1} for C-O-C, 1750cm^{-1} for C=O and 3000cm^{-1} for CH groups. Chemical structure of PLCL was embedded on the spectrograph.~~ ~~**(B)**~~ Cytotoxicity using human MSCs as model for human application (i) Metabolic activity and (ii) cell number with MSC cultured in direct contact with the construct or using construct conditioned medium (elution) compared to cells cultured on tissue culture plastic as a control. Data is presented as mean ± SEM, n=3, $p>0.05$.

Figure 3 (A) Representative images of colony formation (i) in control culture medium or (ii) in culture medium with 2% rabbit serum (rabbit serum) demonstrating an increase in CFU-F in rabbit serum supplemented medium. **(B)** Number of colonies formed, revealing a statistically greater number of colonies formed in the presence of the rabbit serum **(C)** Growth of rabbit MSCs was significantly increased by the

addition of 2% rabbit serum higher and **(D)** morphological images at passage 2 revealing that (i) larger flat cells with a senescent phenotype were visible in the absence of serum, as indicated by the black arrows, while (ii) cells cultured in the presence of rabbit serum have a typical fibroblastic appearance (scale bar 20 µm).

Figure 4~~(E)~~ Representative images showing tri-lineage differentiation of rabbit MSCs. Cells induced to undergo adipogenesis showed reduced oil red O staining in the cells sub-cultured in the (i) absence of rabbit serum (rabbit serum) compared to (ii) cells sub-cultured in the presence of 2% rabbit serum (scale bar 200 µm). Calcium deposition indicative of osteogenesis, as detected by alizarin red staining, was also decreased in (iii) cells sub-cultured without rabbit serum compared to (iv) cells sub-cultured in the presence of 2% rabbit serum (scale bar 500 µm). There was no evidence of chondrogenesis observed in the (v) absence of rabbit serum, while positive toluidine blue staining for GAG was observed (vi) with rabbit serum (scale bar 200 µm).

Figure 5~~4~~ H&E staining showing no adverse tissue response in terms of inflammation or giant cells in the empty defect, the cell-free construct or the rabbit MSC-seeded construct, at 4x, 10x and 20x objective lens magnification, with scale bar lengths of 1000 µm, 500 µm and 200µm respectively. Dotted black box shows original defect site areas and s denotes the scaffold.

Figure 6~~5~~ (A) Toluidine blue staining showing absence of chondrogenesis in the empty defect and evidence of integration, GAG accumulation and chondrocytes in the cell-free PLCL construct. ~~Although the rabbit MSC-seeded scaffold stained positive for toluidine blue, the cells observed are smaller suggesting that they are the rabbit MSCs rather than endogenous cells from the joint such as those observed in~~

~~the cell-free construct.~~ (4x, 10x and 20x objective lens magnification, with scale bar lengths of 1000 µm, 500 µm and 200µm respectively). Black arrows indicate areas of poor scaffold integration and s denotes the scaffold strut.

Figure 7 ~~(B)~~ Collagen type II staining is positive in ~~as indicated by the brown colour in~~ the adjacent tissue of~~in~~ the empty defect and in between and adjacent to the struts in the cell-free construct (brown DAB positive stain together with pink-eosin counterstain). The brown colour as evidence of c~~C~~ollagen type II is less ~~evident~~apparent in and around the struts of the cell-seeded constructs at 4x and 20x objective lens magnification, with scale bar lengths of 1000 µm and 200µm respectively. Collagen type I staining is negative in the adjacent tissue (pink–eosin counterstain) and positive (brown) in the empty defect, in addition to the defects containing the cell-free construct and the rabbit MSC-seeded construct. Dotted box shows the outline of an empty defect, black arrows indicate the presence of collagen type II in the native tissue in the empty defect and the repair tissue in the scaffold containing defects. Red arrows indicate the absence of collagen type I in native cartilage and s denotes the PLCL strut.

Formatted: Font: Bold

Figure 1A Functionally graded pore size

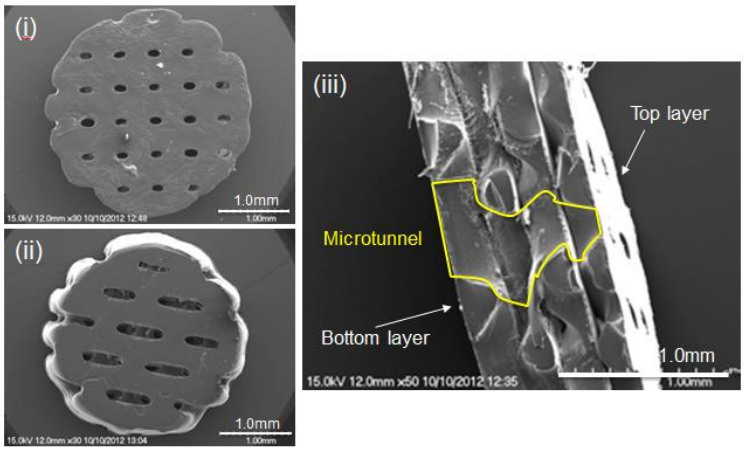

Figure 1B Compressive properties

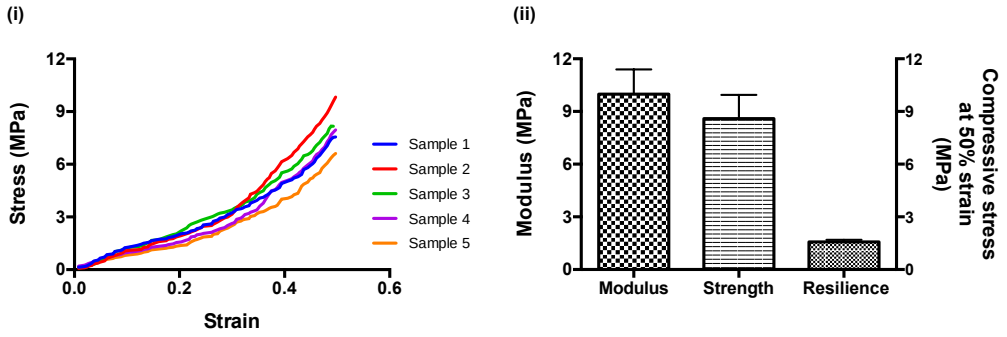

Figure 2 Cytotoxicity post sterilization

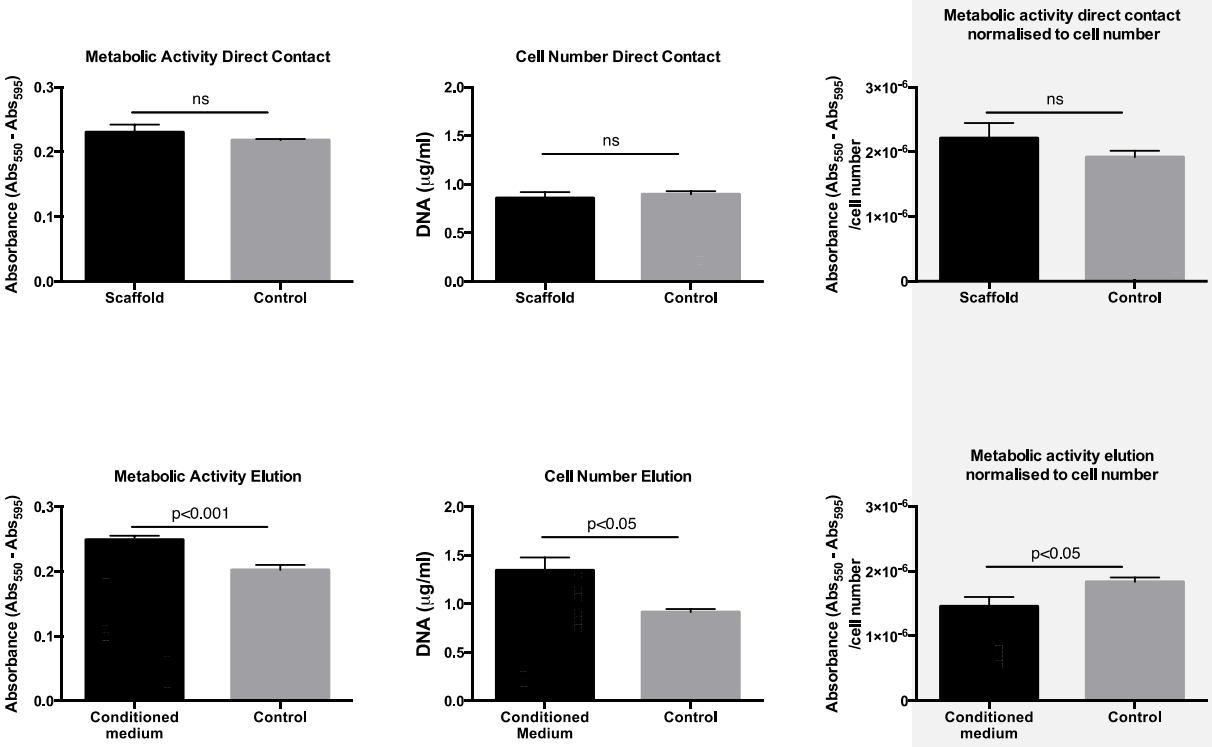

Figure 3 Isolation and characterisation of rabbit MSC

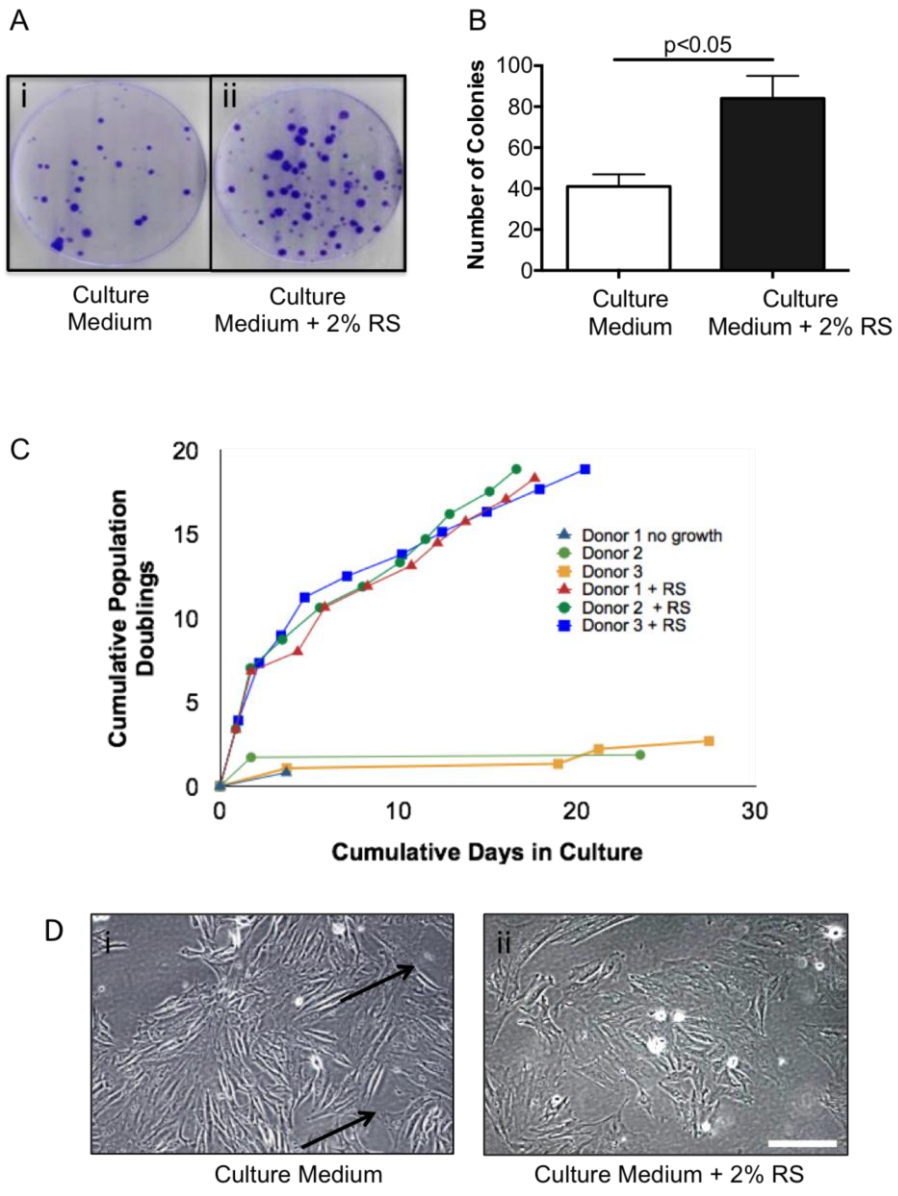

Figure 4 Tri-lineage differentiation of rabbit MSCs

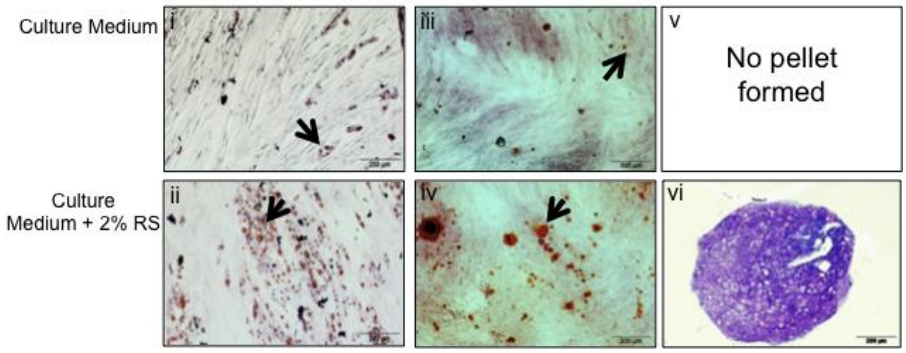

Figure 54 Histological evaluation: H&E staining

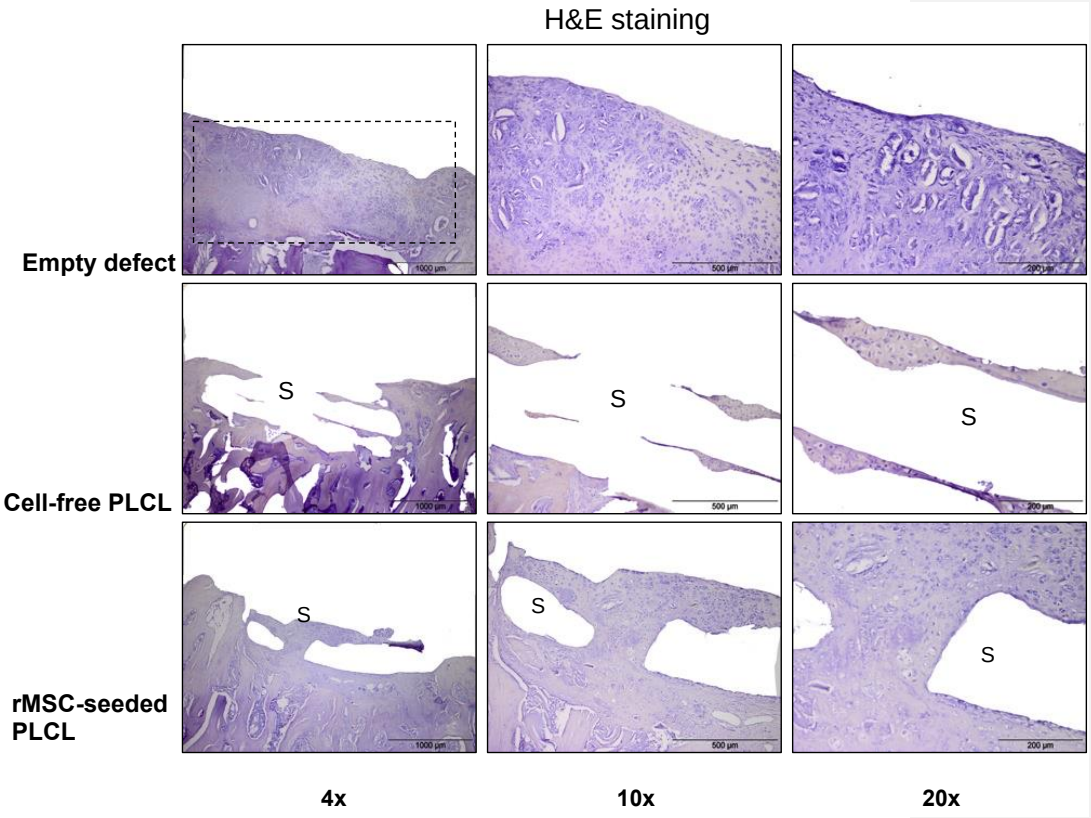

Figure 6~~5A~~ Histological evaluation: toluidine blue staining

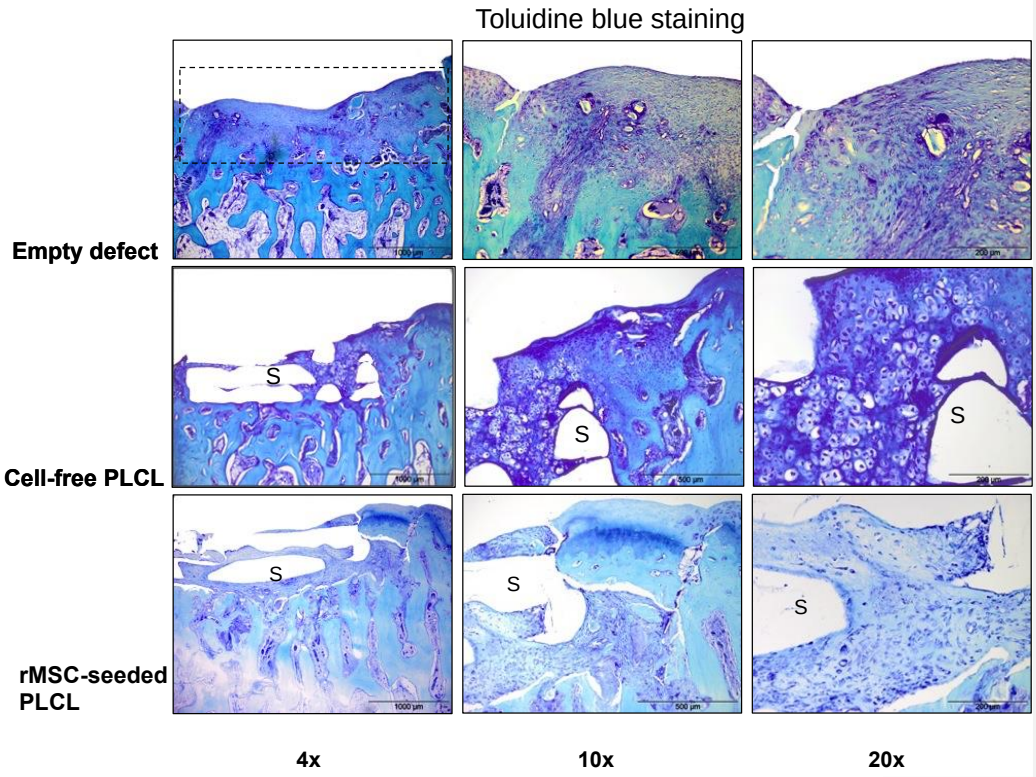

Figure. 7~~5B~~ Histological evaluation: Collagen type II and type I staining

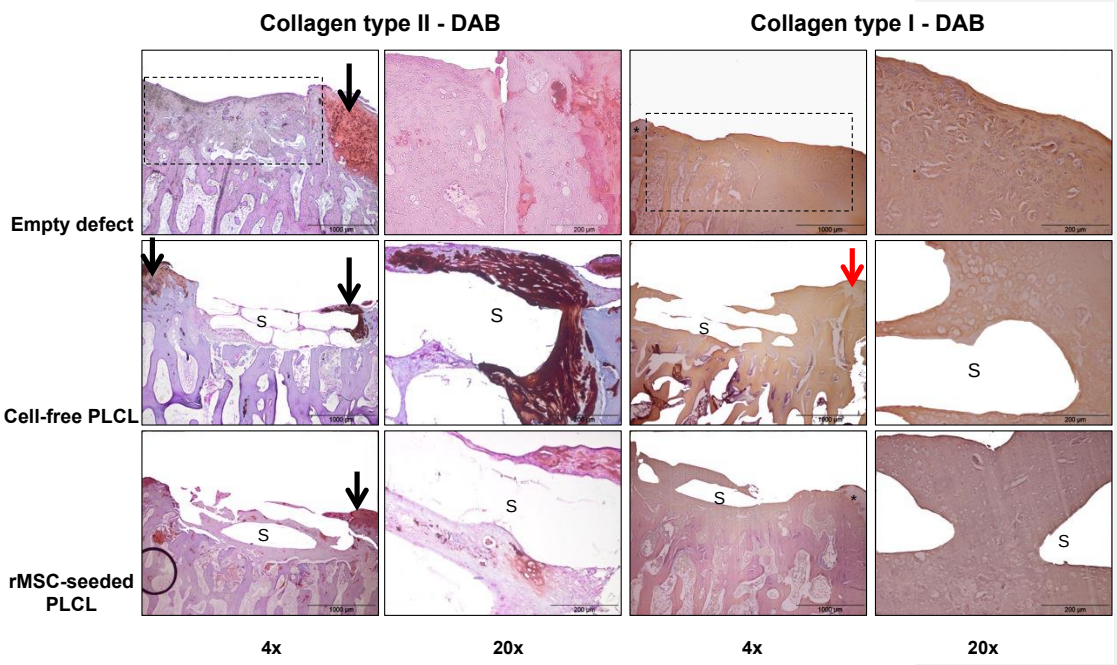

Supplementary information

Chemical properties after sterilization

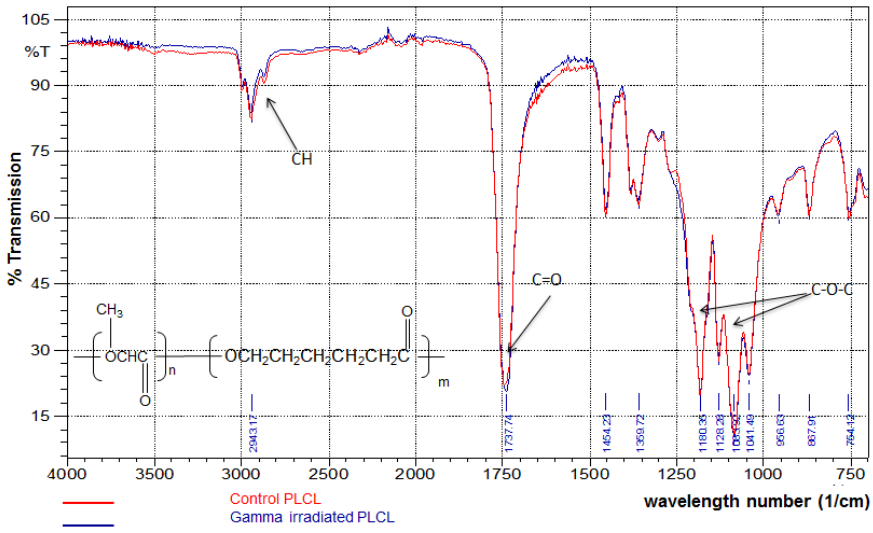

Thermal analysis of PLCL constructs

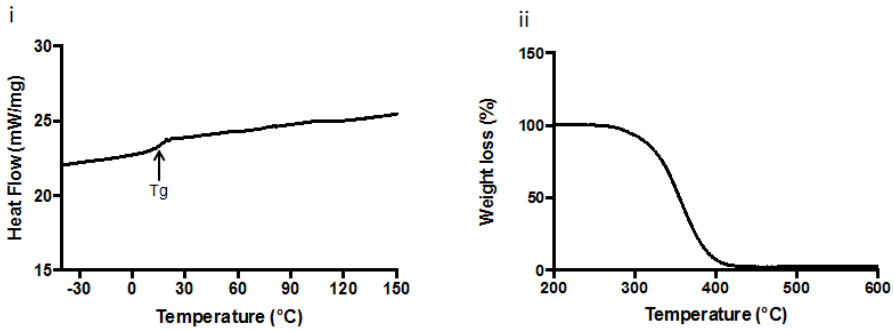

Molecular weight distribution of constructs

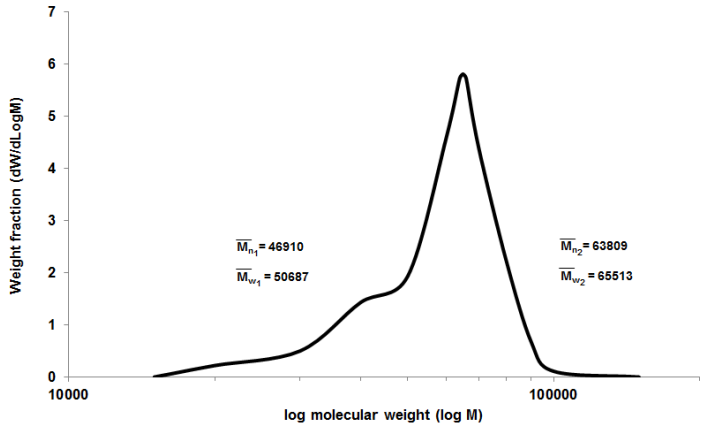

Montage of images stained with toluidine blue for all 18 defects (* indicate same rabbit).

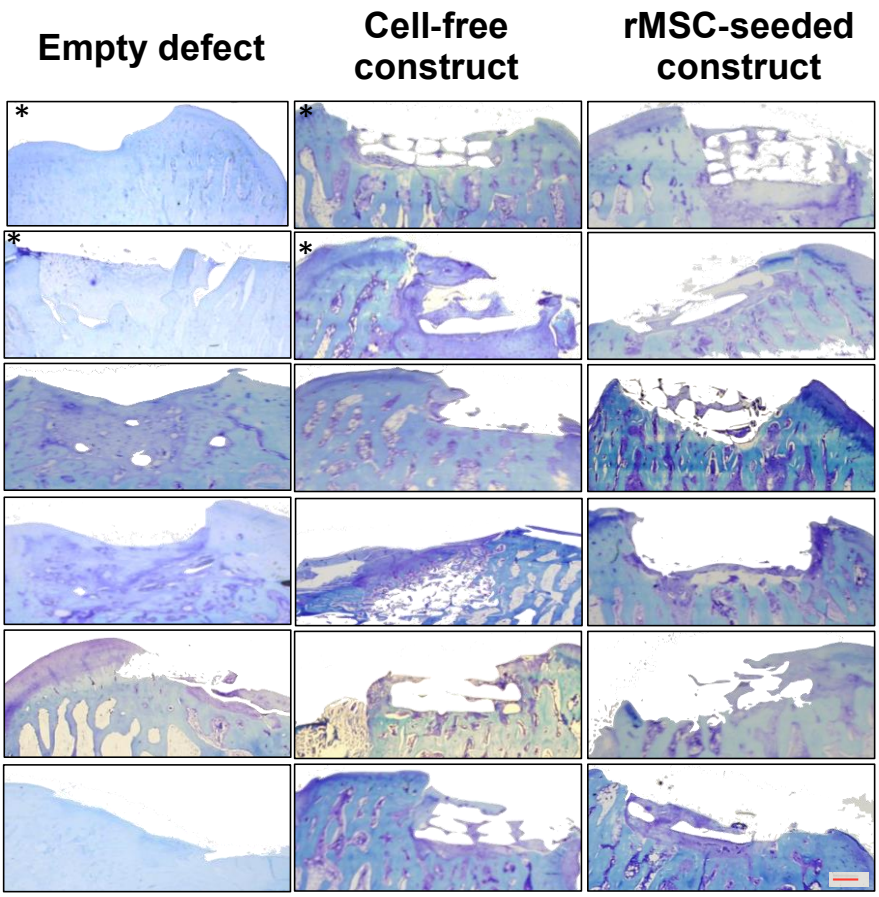

Evaluation of the Early *In vivo* Response of a Functionally Graded Macroporous Scaffold in an Osteochondral Defect in a Rabbit Model

Valerie Barron[1¥], Martin Neary[1], Khalid Merghani Salid Mohamed[1], Sharon Ansboro[1], Georgina Shaw[1], Grace O'Malley[1], Niall Rooney[2], Frank Barry[1], Mary Murphy[1]*

[1]Regenerative Medicine Institute (REMEDI), Biosciences, National University of Ireland Galway, Galway, Ireland

[2]Proxy Biomedical Ltd., Coilleach, Spiddal, Co. Galway, Ireland

***Corresponding author:** Mary.Murphy@nuigalway.ie

[¥]current address: Materials Research Institute, Athlone Institute of Technology, Dublin Road, Co. Westmeath, Ireland.

Abstract

Cartilage tissue engineering is a multifactorial problem requiring a wide range of material property requirements from provision of biological cues to facilitation of mechanical support in load-bearing diarthrodial joints. The study aim was to design, fabricate and characterize a template to promote endogenous cell recruitment for enhanced cartilage repair. A polylactic acid poly-ε-caprolactone (PLCL) support structure was fabricated using laser micromachining technology and thermal crimping to create a functionally-graded open pore network scaffold with a compressive modulus of 10MPa and a compressive stress at 50% strain of 8.5MPa. In parallel, rabbit mesenchymal stem cells (MSC) were isolated and their growth characteristics, morphology and multipotency confirmed. Sterilization had no effect on construct chemical structure and cellular compatibility was confirmed. After four weeks implantation in an osteochondral defect in a rabbit model to assess biocompatibility, there was no evidence of inflammation or giant cells. Moreover, acellular constructs performed better than cell-seeded constructs with endogenous progenitor cells homing through microtunnels, differentiating to form neo-cartilage and strengthening integration with native tissue. These results suggest, albeit at an early stage of repair, that by modulating the architecture of a macroporous scaffold, pre-seeding with MSCs is not necessary for hyaline cartilage repair.

Keywords: Functionally Graded; Polylactic Acid-ε-Polycaprolactone, Cartilage Repair, Integration, Neotissue formation

Introduction

Once damaged by osteoarthritis or trauma, self-repair/regeneration of articular cartilage is limited. Current medical treatments include debridement, marrow stimulation using microfracture techniques and osteochondral grafting. Although in the shorter term, these techniques improve mobility and alleviate pain, fibrous cartilage does not possess the optimal biological and mechanical properties to provide a long-term solution.[21] More recently, autologous chondrocyte implantation (ACI), a cell-based therapy, which involves the implantation of expanded autologous chondrocytes under a periosteal patch, has demonstrated improvement in function, reduction in pain and some hyaline cartilage regeneration. However, this technique has not been readily adopted due to cost, technical challenges associated with surgery and post-surgical complications with the periosteal patch.[3] This in turn has led to the development of cell-free membranes such as Chondro-gide® and cartilage treatment options such as the Cartilage Autograft Implantation System (CAIS) and deNovo natural tissue (deNovoNT®).[6] Since its introduction, matrix-induced autologous chondrocyte implantation, or MACI has produced optimistic yet mixed results in clinical trials,[22] leading to the European Medical Agency requesting 5-year follow-up data to allow a better comparison with microfracture over time for marketing authorisation.[5] Nonetheless, it is designed as a periosteal flap replacement to retain autologous chondrocytes at the site of injury rather than providing a biomimetic support structure for endogenous cell recruitment. Development of advanced functional biomaterials to recruit host stem cells to promote regeneration and repair of articular cartilage may represent a biomedical engineering-based alternative to current strategies for repair of articular cartilage defects.

Over the past 20 years, tissue-engineering strategies have been developed for the repair and regeneration of damaged articular cartilage. Early attempts focused on the development of a range of degradable polyester constructs such as polylactic acid (PLA), polyglycolic acid (PGA) and polylactic acid glycolic acid (PLGA) meshes and sponges with design criteria such as pore interconnectivity, porosity and degradation rate investigated for optimal cell viability and neotissue integration.[7,8,11] However, *in vivo* cartilage repair was not optimal and it was suggested that better repair could be achieved by tailoring the mechanical properties of constructs to mimic the native mechanical properties of articular cartilage.[27] In terms of identifying the exact mechanical property requirements for native cartilage, large variations can be observed in the literature due to differences in donor age, tissue isotropy, biochemical composition and state of degeneration. Nonetheless, using computational analysis, it was found that the optimal elastic modulus for a construct for osteochondral repair lies between 1 and 50MPa; above or below these values cartilage formation decreased, while fibrous tissue and bone formation increased.[18] Moreover, it was also revealed that the optimal compressive modulus for functional tissue support was in the region 1-12MPa.[12] Using this approach, Malda *et al.* developed a polyethylene terephthalate/polybutylene terephthalate (PEOT/PBT) polymer with a finely-tuned biochemical composition and dynamic stiffness values matching that of native cartilage.[23] Although the chemical composition had been custom-made for cartilage applications, the architecture of the construct lacked depth-dependent mechanical properties. In an effort to overcome this limitation, Lee *et al.* developed a cell-free polycaprolactone (PCL)-based construct with a functional graded pore architecture with 400μm pores on the top surface through to 200μm pores on the bottom surface that displayed promising cartilage repair *in vivo*.[19] More

recently, Mendoza-Palomares *et al.* developed a smart hybrid system equipped with nanoreservoirs of therapeutic agents, which promoted cartilage repair in an osteochondral defect.[24] These studies present an alternative approach to that of scaffolds seeded with cells to promote hyaline cartilage repair. Not only will waiting periods associated with cell harvesting and expansion for ACI and MACI be reduced but just one surgical intervention will be required.

In parallel, other researchers have begun to investigate the effect of polymer degradation rate on the inflammatory response of medical implants *in vivo*, where it has been shown that biocompatibility is improved in the presence of slowly degrading materials.[13] In particular, the first 28 days in the repair process are critical[9] as undesirable polymer degradation products can provoke an inflammatory response and adversely affect the repair process. We hypothesized that by striking a balance between pore architecture, mechanical properties and degradation rate of the scaffold, enhanced repair could be achieved. Specifically, the main objectives of this study were (1) to fabricate 3D porous constructs with an open tunnel network and mechanical properties similar to those proposed by previous studies[18] and (2) to examine inflammation and early chondrogenic response in an defect in a rabbit model.

Materials and Methods

Materials

All materials were purchased from Sigma Aldrich, Dublin, Ireland unless specified.

Scaffold fabrication

Based upon the materials property requirements described above, a 70:30 polylactic acid poly-ε-caprolactone (PLCL) copolymer with an intrinsic viscosity midpoint of 1.5 dl/g (PURASORB PLC7015, Purac Corbion, Amsterdam, The Netherlands) was selected as the material for the construct. Using laser micro-machining technology in combination with thermal crimping a 3D porous substrate with a functionally-graded pore structure was created to mimic the orientation and distribution of cells in native hyaline cartilage.

Physical characterisation of the scaffold

The 3D architecture of the PLCL construct was imaged using micro computed tomography (SCANCO Medical AG Bassersdorf, Switzerland) high resolution scans, with a resolution of 6 microns using 70 kVp, 114 μA and 8 Watts. In parallel, the open pore tunnel structure was visualized using scanning electron microscopy (SEM) (Hitachi, S4700, UK). In brief, samples were sputter coated with gold and imaged using a 15kV accelerating voltage for analysis of pore size, pore shape and open microtunnel observation. Additionally, to ensure reproducibility and reliability of the fabrication methods, the polymer morphology and molecular weight was examined using differential scanning calorimetry, thermal gravimetric analysis and gel permeation chromatography (See supplementary data).

Mechanical testing

Compression testing was performed on as-fabricated dry samples on a Zwick mechanical testing machine (Zwick, UK) at room temperature using a load cell of 100N and a crosshead speed of 10mm/min according to ASTM-D695-10 (n=5). An

initial tare load of 0.2 N was applied to the sample. Stress strain curves were generated from which it was possible to determine the elastic compressive modulus from the slope of the linear region, the compressive stress at 50% strain and the resilience from the area under the curve.

Sterilization

After fabrication, the PLCL scaffolds were sterilized by gamma irradiation using a 25kGy dose. To ensure that there was no change in the chemical properties of the scaffolds, the chemical structure was analyzed using Fourier transform infra-red spectroscopy (FTIR-8300, Shimadzu, UK). Spectra were recorded in the wavelength range 4000cm^{-1} to 400cm^{-1} by 2cm^{-1} resolution in 32 scans and in 10 different areas for each specimen (n=6). In addition, cytotoxicity test methods were conducted in accordance with ISO 10993-12 to examine the cell response after sterilization, using human bone-marrow derived MSCs as a cell source, since the ultimate application was for human use. In brief, the MSCs at passage 3 (n=3 technical replicates from one male donor aged 24) were seeded at a density of 2 x 10^4 cells/cm^2 and maintained for 24h at 37°C in a humidified atmosphere and 5% CO_2. In parallel, the constructs were immersed in MSC culture medium [α-minimum essential medium (α-MEM, Gibco, Thermo Fisher, Dublin), 10% fetal bovine serum and 1% penicillin/streptomycin] to create conditioned medium After 24h the PLCL constructs were placed on the cells for direct contact analysis, while the conditioned medium was used in parallel for MSC growth (n=6). An AlamarBlue™ assay (Lifescience Technologies, Thermo Fisher, Dublin) was employed to examine MSC metabolic activity after 72h by measuring the absorbance at 550nm and 595nm. Cell number was also assessed using a PicoGreen dsDNA quantification fluorescence assay

(Lifescience Technologies, Thermo Fisher Dublin) (485nm excitation/535 nm emission) on a plate reader. As a method of control MSC were seeded on tissue culture plastic.

Isolation and characterization of rabbit mesenchymal stem cells

To assess the early repair response *in vivo*, MSC were obtained from the tibia of skeletally mature male (>3kg) New Zealand white rabbits (Charles River, France) (n=6). All procedures including bone marrow harvest were conducted with approval from the National University of Ireland Galway's Animal Care and Research Ethical Committee. A disposable 18-gauge intraosseous infusion needle was used to access the bone marrow compartment in the tibia with radiographic guidance (GE OEC 9800 Plus) under anaesthesia. Bone marrow (5ml) was aspirated into a syringe containing 1ml heparin diluted to 3,000units/ml in saline and transferred to a 50ml sterile tube. Bone marrow aspirates were washed with Dulbecco's phosphate buffered solution (D-PBS) and filtered using a 70µm cell strainer. Mononuclear cells (MNC) were cultured at 37°C in 5% CO_2 and a humidified atmosphere at a density between 100,000 – 115,000 cells/cm^2 in control culture medium (α-MEM. Gibco-UK) containing 10% fetal bovine serum and 1% penicillin/streptomycin (P/S), enriched medium with 2% rabbit serum (R4505, Sigma, Dublin,).Once confluent, cells were detached using 0.25% trypsin/EDTA for 5 min at 37°C and passaged at a density of 5,500 cells/cm^2. Cell morphology was observed using light microscopy (Olympus IX71 microscope). CFU-F assays were conducted for each marrow with 3 x 10^6 MNCs cultured in 10cm tissue culture dishes (n=3 for 2 donors) until discrete colonies were observed. Medium was removed and colonies fixed with 90%

methanol prior to staining with 2% crystal violet (C0775, Sigma, Dublin) The dishes were imaged using a flatbed scanner (Epson Stylus Sx425W) and the number of colonies quantified using ImageJ analysis. Growth kinetics of the rabbit MSC cultures with or without 2% rabbit serum were evaluated over a 30-day cell culture period by calculating the cumulative population doublings. Thereafter, tri-lineage differentiation was examined using methods previously described.[25] For adipogenesis, confluent cultures were exposed to induction medium (DMEM high glucose (HG-DMEM), 10% FBS (Hyclone, Logan, UT, USA), 1% P/S, 10µg/ml insulin, 1µM dexamethasone, 500µM isobutylmethylxanthine and 200µM indomethacin) for 3 days, followed by 1-3 days in maintenance medium (DMEM high glucose, 10% FBS, 1% P/S and 10µg/ml insulin). The cycle was repeated 3 times with cells left in maintenance medium for 7 days in total prior to harvesting for analysis. At the end of the culture period, medium was removed and the cells washed twice in D-PBS prior to fixation in 10% neutral buffer formalin for 20 min. The fixative was removed and cells exposed to 0.2% Oil Red O for 5 min. Excess stain was removed with isopropanol and cells counterstained with haematoxylin. Images were acquired using the Olympus Ix71 microscope. After visualization, the oil red O was extracted with 100% isopropanol and the absorbance measured at 520nm to determine the total bound oil red O per well.

In the case of osteogenesis, the MSCs were plated in a 6-well plate at density of 2 x 10^4 cells/cm^2 and treated with osteogenic medium (Dulbecco's modified Eagle's medium (DMEM) low glucose, 10% FBS, 1% P/S, 0.1µM dexamethasone, 50µM ascorbic acid 2-phosphate and 10mM β-glycerophosphate) for 14-17 days. The osteogenic medium was replaced every 3 days and harvested after 14 days culture.

Following careful washing with PBS, the cells were scraped and transferred into 1ml of 0.5M HCl and placed in an orbital shaker at 4°C overnight. After centrifugation, the debris was removed and the calcium concentration was determined using a Stanbio Calcium (CPC) LiquiColor® Test Kit (Lonza, UK). The calcium solution in the kit was used to generate a standard curve from which it was possible to determine the calcium concentration from the absorbance measured at 550nm on a microplate reader (FLX800, Biotek Instruments Inc.). Calcium deposition was also assessed visually using Alizarin Red S: medium was removed and cells fixed in ice cold 95% methanol for 10 min after washing twice with D-PBS. After rinsing in distilled water, the plate was stained with a 2% Alizarin Red S solution for 5 min. Calcium deposits were visualised and imaged using light microscopy (Olympus IX71 microscope).

For chondrogenesis, 2.5 x 10^5 rabbit MSCs were cultured in complete chondrogenic medium (CCM) consisting of G-DMEM supplemented with 100nM dexamethasone, 50µg/ml ascorbic acid, 40µg/ml L-Proline, 6.25µg/ml selenous acid, 5.33µg/ml linoleic acid, 1.25mg/ml bovine serum albumin, 0.11mg/ml sodium pyruvate, 1% P/S and 10ng/ml transforming growth factor (TGF)-β3) with medium changed every 2 days. After 21 days in pellet culture, the cell culture medium was removed and the pellets were washed twice with D-PBS, fixed with 10% neutral buffer formalin for 20 min and washed again with D-PBS. The fixed pellets were dehydrated in a series of alcohols from 50% to 100% and infiltrated with paraffin (Leica EG/550H wax embedder). Thereafter, the samples were de-paraffinized using xylene and rehydrated in alcohol. Sections were stained with 1% toluidine blue for 5 min at 60°C. Images were acquired using a digital camera and Olympus BX51 Upright

Fluorescent Microscope with Improvision Optigrid System linked to camera microscope.

Animal surgery

Nine skeletally mature male New Zealand white rabbits, weighing more than 3kg were used in this study to evaluate biocompatibility and early repair. Both knees in each rabbit underwent surgery under sterile conditions. In total 18 knees were randomly assigned into three groups, including empty defect (n=5 knees, with 6 technical replicates - one rabbit received two empty defects, one in the left knee and one in the right as a result of the randomization), cell-free constructs (n=5 knees, with 6 technical replicates - one rabbit received two cell-free constructs, one in the left knee and one in the right as a result of the randomization) and MSC-seeded constructs (n=6 knees). Briefly, the rabbits were anaesthetized using a weight-adjusted dose of ketamine (35mg/kg) and xylazine (10mg/kg). The operative leg was secured in a retort stand and access to the knee joint achieved via an anterior midline skin incision, followed by a medial para-patellar joint capsule incision. The patella was dislocated laterally to provide increased exposure of the medial femoral condyle. To facilitate testing of these constructs, which were custom designed for human chondral defects with dimensions of 3mm in diameter and 1mm in height, a 1mm shallow osteochondral defect was created on the medial femoral condyle using a drill with a previously sterilized 2.8mm drill bit covered with a sterile depth stop. The walls of the defect were finished with a dental curette, and the constructs were press-fit into place. The cell-seeded constructs were cultured in serum-free cell culture medium (HG-DMEM supplemented with 100nM dexamethasone, 50µg/ml ascorbic acid, 40µg/ml L-Proline, 6.25µg/ml selenious acid, 5.33µg/ml linoleic acid,

1.25mg/ml bovine serum albumin, 0.11mg/ml sodium pyruvate, 1% penicillin/streptomycin) for 24h prior to surgery, using a cell seeding density of $1.2X10^6$ syngeneic rabbit MSC (passage one) per construct as previously described.[17]

Histological staining for inflammation

After 4 weeks, the rabbits were sacrificed and post examination of gross surface morphology the femoral condyles were removed and fixed in 10% neutral buffered formalin for 10 days as previously described.[29] Following fixation, samples were decalcified in Surgipath® for 2-3 weeks, with solution changes every 3 days. Decalcification was deemed to be complete following 2 consecutive negative tests for residual calcium using equal volumes of 5% ammonium oxalate and 5% ammonium hydroxide and decalcifying solution. After processing and paraffin embedding, histological sections (5μm) were dewaxed at 65°C, immersed in histoclear and rehydrated in a series of alcohols 100%, 95% and 70% prior to staining with H&E for assessment of an inflammatory response. Briefly, sections were exposed to Harris hematoxylin for 7 min, blued in Scott's tap water substitute for 2 min and counterstained with eosin Y for 7 min.

Staining for early chondrogenesis and repair

Sections were stained for evidence of early chondrogenesis using toluidine blue (TB). Positive collagen type II immunostaining was used to assess the presence of hyaline cartilage and collagen type I used to assess fibrous cartilage. For collagen type I and II immunostaining, an endogenous hydroxide quench was performed with

0.3% hydrogen peroxide (H_2O_2) in methanol after rehydration. Thereafter, antigen retrieval was performed using pepsin (DAKO, S3002 4% in 0.2N HCl, Agilent Technologies, Dublin) for 30 min, followed by blocking with 5% rabbit serum in tris-buffered saline (TBS 0.05M tris, 0.15M NaCl, pH 7.6) for collagen type I and 10% goat serum (KPL 71-00-27, Insight Biotechnology, Middlesex) in TBS for collagen type II. Sections were incubated overnight at 4°C with goat polyclonal anti-type I collagen antibody (1:100, S1301-01, Southern Biotech, Birmingham, AL, USA,) and with mouse monoclonal anti-rabbit type II collagen antibody (1:50; AF5710, Acris,Herford, Germany). Sections were then incubated with biotinylated secondary antibodies against rabbit anti-goat (H+L) (1:1000; 305-065-003 Jackson ImmunoResearch, Newmarket) for collagen type I or goat anti-mouse (H+L) (1:1000; KPL 71-00-29, Insight Biotechnology, Middlesex) for collagen type II followed by peroxidase-conjugated streptavidin (KPL 71-00-38) at room temperature for 30 min each and stained for visualization with 3,3' diaminobenzidine (DAB) (Abcam, substrate kit, ab94665, Cambridge, UK). Sections were counterstained with Harris hematoxylin for 10 sec and eosin-phloxine B for 1 min. After staining, all sections were dehydrated in a series of alcohols (70%, 95% and 100%), cleared with histoclear and mounted using histomount for imaging using the Olympus BX51 Upright Fluorescent Microscope.

Statistical Analysis

Compressive property data are expressed as means ± standard error of the mean (SEM). Colony formation and cytotoxicity studies were analyzed using a student's t

test with p≥0.05 considered not significant (ns). All data was analysed using GraphPad Prism version 6.

Results

3D construct with open pore microtunnel structure

A biomimetic architecture was created by a combination of laser machining and precise offsetting of the various layers resulted in an open pore structure, with microtunnels visible from the top surface through to the bottom (Fig. 1 and supplementary video). Using SEM (Fig. 1), it can be seen that the pore size increases from 180μm in diameter at the top (Fig. 1Ai) to 200μm X 600μm at the bottom surface of the construct (Fig. 1Aii) creating an open tunnel through the structure (Fig. 1Aiii).

Compressive properties of the 3D scaffold

The stress strain curves generated from the compression test are shown in Fig. 1Bi, where it can be seen that a similar curve was generated for each sample and that the PLCL constructs had a mean compressive modulus of 10 ± 1.41 MPa, a mean compressive stress at 50% strain of 8.5 ± 1.35 MPa and a mean recoverable elastic energy per unit volume that can be stored in the polymer or modulus of resilience value of 1.5 ± 0.12 MPa (Fig. 1Bii)

Sterilization

Sterilization by gamma irradiation did not affect the chemical structure of the PLCL copolymer with no difference observed in the characteristic PLCL peaks at 1050-

1180cm^{-1} for C-O-C, 1750cm^{-1} for C=O and 3000cm^{-1} for CH groups using FTIR spectroscopy (see supplementary figure). The metabolic activity of human MSCs was examined for cells cultured in direct contact with the scaffold and using conditioned medium (Fig. 2). As shown in Fig. 2i, Fig. 2ii and Fig. 2iii, there was no statistically significant difference observed in metabolic activity, cell number or normalized metabolic activity per cell number for cells grown in the presence of the PLCL construct. In contrast, a significant difference was observed in metabolic activity (Fig. 2iv), cell number (Fig. 2v) and normalized metabolic activity per cell number (Fig. 2vi) for cells grown in conditioned medium, where a 19% increase in metabolic activity, a 32% increase in cell number and a 26% decrease in normalized metabolic activity per cell number was observed.

MSC growth characteristics

As shown by crystal violet staining in Fig. 3A, rabbit MSCs did not form colonies efficiently in the absence of 2% rabbit serum. Quantification of CFU-F data indicated double the number of colonies in supplemented cultures, with average values of 40 recorded without and values of over 80 recorded in the presence of 2% rabbit serum (Fig. 3B). In terms of cumulative population doublings, the cells did not proliferate in the absence of rabbit serum after P0 (Fig. 3C). Moreover, the cells did not maintain their characteristic MSC morphology and were much larger and flatter in the absence of rabbit serum (Fig. 3Di, black arrows).

Tri-lineage differentiation of rabbit MSCs

The differentiation potential of the rabbit MSCs was examined with and without 2% rabbit serum (Fig. 4), with oil red O staining confirming the presence of adipocytes

(Fig. 4i, ii), calcium deposition providing evidence of osteogenesis (Fig. 4iii, iv) and GAG accumulation as illustrated by positive staining for toluidine blue providing evidence of chondrogenesis (Fig. 4vi). Differentiation was observed in all cases in the presence of 2% rabbit serum, with oil red O (Fig. 34i,ii) and calcium deposition (Fig. 4iii, iv) highlighted with the black arrows, where it can be seen that both adipogenesis and osteogenesis is much more evident in the presence of the serum. Moreover, in the absence of rabbit serum, the rabbit MSCs were unable to condense and form a pellet, while in the presence of 2% rabbit serum chondrogenesis was observed in the pellet shown in Fig. 4(vi).

Inflammation and biocompatibility

Hematoxylin and eosin (H&E) staining was used to evaluate whether there was an adverse effect to the surrounding tissue after 4 weeks implantation. As expected, tissue fill was observed for the empty defect, highlighted by the box with dotted lines. However, there was no evidence of inflammation or giant cells in the cell-free construct or the cell-seeded construct in the representative images shown in Fig. 5.

Assessment of chondrogenesis and early repair

Evidence of chondrogenesis, neo-tissue formation and integration was examined using toluidine blue staining. In the montage of images from all defects shown in the supplemental figures, fibrous tissue fill can be seen in three of the empty defects, with the other three defects remaining empty. In comparison, four of the defects containing cell-free constructs revealed evidence of cartilaginous neotissue formation in and around the struts of the scaffold, with two defects appearing to

remain empty. A similar trend was observed for the cell-seeded scaffolds, with only two defects appearing empty. As shown in Figure 6, lateral integration with native cartilage in the empty defect was observed to be incomplete as highlighted by the black arrow. In contrast, it can be seen that there was evidence of integration between the host tissue and the cell-free construct. At lower magnification, the scaffold appeared to be integrated at the bottom and at both sides of the defect and lateral integration with host tissue is emphasized in the 10x representative image. Of relevance is the appearance of round, toluidine blue-positively stained cells with a chondrocytic morphology seen at 20x, suggesting that the underlying bone marrow diffused in and around the scaffold struts, resulting in early chondrogenesis. With respect to the cell-seeded construct, the sections also stained positive for toluidine blue, but there was less evidence of neo-tissue organization or integration as indicated by the black arrow.

Regarding hyaline cartilage repair, collagen type II staining was observed in and around the struts of the cell-free construct; while there was much less evidence of collagen type II in the rabbit MSC-seeded scaffold and no collagen type II in the empty defect (Fig. 7). However, there was evidence of collagen type I staining in all three defects. On closer examination of the cell-free construct (20x), the immature chondrocytes visible around the struts did not stain positive for collagen type I (Fig. 7).

Discussion

In a recent study by Lee *et al.*,[19] it was suggested that a functionally-graded pore architecture promoted endogenous cell recruitment and provided a superior support

structure for cartilage repair. To achieve this specific functionality, a support structured was designed and fabricated to mimic both the structure and mechanical properties of native articular cartilage repair. Fig. 1A illustrated the generation of a biomimetic pore structure, with an open tunnel system, created by the custom-designed layer structure. In addition to creating an open functionally-graded pore template for cells that complements the work of Chou *et al.*[4] and Lee *et al.*,[19] the compressive modulus values were orders of magnitude higher (10 MPa) than previous composite constructs[27] (0.005-0.10 MPa) and represent a step towards mechanical property values proposed for hyaline cartilage regeneration in the region 1-12MPa.[12] However, it must be noted that compression testing of the macroporous PLCL scaffolds was performed on dry samples at room temperature and that future studies will be conducted to examine the mechanical properties of constructs stored in simulated physiological solutions at 37°C to allow better comparison with the mechanical properties of cartilage in addition to examining the changes that occur over time.

Regarding sterilization, there were no changes observed in the chemical structure of the polymer post gamma irradiation. In terms of *in vitro* cell response, cells exposed to conditioned medium were healthy and proliferated well with significantly increased metabolic activity and cell number compared to control cells. When metabolic activity was normalised to cell number, the data did suggest a minimal negative effect of the conditioned medium that did not translate to a biological effect, as the cells were metabolically active and the chemical structure of the polymer was unaltered. This is in line with Wang *et al.*, where low concentrations of polymer eluates in conditioned medium were shown to increase cell numbers without adversely affecting cell

viability or biocompatibility[30] of ultra-high molecular weight polyethylene for hip joint applications.

Previous studies successfully employed bone marrow-derived MSCs for cartilage repair applications. In a recent publication, it was revealed that rabbit MSCs became senescent when expanded in culture.[24] In an effort to overcome this limitation, rabbit cells were cultured in cell culture medium containing 2% rabbit serum. To ensure the MSCs retained their plasticity, tri-lineage differentiation assays were performed. As shown, the cells retained their MSC characteristics, did not lose their tri-lineage potential as described by Ahmadbeigi *et al.*,[1] when cultured in the presence of 2% rabbit serum. These assays confirmed the phenotype of the optimized rabbit MSC preparations *in vitro* and validated their use *in vivo*.

In relation to limitations of the animal study, the number of replicates is noted. Due to the randomization, one rabbit received two empty defects, one in the left knee and one in the right and another rabbit received two cell-free constructs, one in the left knee and one in the right. As shown in montage of images in the supplemental figures, there was no trend for repair in the rabbit that received an empty defect in both knees, with one knee remaining empty and the other showing evidence of tissue fill, albeit fibrous tissue formation. With respect to the rabbit that received two cell-free constructs, there is evidence of neotissue formation and chondrogenesis in both knees. The number of specimens analyzed was sufficient to compare biocompatibility and early repair, but larger numbers of rabbits, with different test groups in different knees are required for the 12-week cartilage repair proof of principle studies recommended by the International Society for Cartilage Repair (ICRS).[10]

Regarding inflammation, the PLCL scaffold was biocompatible with no evidence of inflammation or giant cells in or around the struts of the template after 4 weeks implantation, which agrees well with previous studies by Jung *et al.*,[15,16] where PLCL was also shown not to evoke an adverse inflammatory response *in vivo*. On first observation, it appeared that the tissue repair in the empty defect was better than that of the scaffolds. However, on closer examination, it was seen that the repair tissue was fibrous primarily, as evidenced by the presence of collagen type I staining and the absence of collagen type II staining. Moreover, there was evidence of chondrocyte clustering and hypo- and hyper-cellularity in the repair and native tissues adjacent to the empty defect, which compared well with previous findings where fibrous tissue formation was observed in empty defects and is perhaps why empty defects, are accepted as a negative control .[2,10] Of more interest was the fact the functionally-graded pore structure appeared to go one step forward compared to Jung[15,16] and enhanced endogenous cell recruitment, integration and neotissue formation, with immature chondrocytes and collagen type II staining visible throughout and under the cell-free PLCL construct. This correlates well with other studies, where cartilage repair was attributed to cell homing, engraftment and repair due to pore architecture of the construct used.[4,9,19] Despite that collagen type I staining was observed in all defects in the present study, chondrocytes adjacent to the cell-free construct did not stain positive. Although, collagen type I is associated with fibrocartilage repair, spatial and temporal patterns of collagen type I expression have been observed during cartilage development,[26] at early time points during *in vitro* chondrogenesis of MSC[14] and after ACI in humans.[20] Therefore, longer time points are required to determine whether the collagen I staining observed in this study occurred as a result of early hyaline cartilage or fibrocartilage development.

The addition of the MSC to the PLCL construct did not appear to enhance hyaline cartilage formation. The immature chondrocytes visible in the cell-free construct were not as evident and lateral integration with native tissue did not appear to be as good as the cell-free construct, which correlated well with the previous studies where the presence of MSCs was believed to impair cell homing and better cartilage repair.[9,28] Since the materials properties and architecture of the functionally-graded scaffold are promising, these results suggest that instead of altering the surface chemistry, mechanical properties or pore architecture as a next step, proof of principle studies such as that recommended by the ICRS with larger numbers and longer time points should be conducted as they would provide very valuable information on the repair potential.

In summary, by tailoring the mechanical properties and pore architecture of a cell-free PLCL construct, microtunnels were created that allowed endogenous cell recruitment, neo-tissue formation and integration. The creation of a cell-free bio-functional material that promotes self-repair and regeneration presents an exciting opportunity to develop a clinically viable one-step surgical intervention for diseased or damaged hyaline cartilage.

Acknowledgements

The authors would like to acknowledge the help of Ms. Teresa Jungwirth, Regenerative Medicine Institute, NUI Galway and Dr. Declan Devine, Athlone Institute of Technology for his help with differentiatal scanning calorimetry. The authors acknowledge the facilities and technical assistance of the Dr. Cathal O'Flaharta at the NCBES Preclinical Facility Core, National University of Ireland Galway. The research leading to these results has received funding from the

European Union's 7th Framework Programme under grant agreement no. HEALTH-2007-B-223298 (PurStem), Science Foundation Ireland (grant number 09/SRC/B1794), Wellcome Trust Biomedical Vacation Scholarships grant number WTD004448 and the Irish Government's Programme for Research in Third Level Institutions, Cycles 4 and 5, National Development Plan 2007-2013.

Competing interest

All authors report no conflict of interest for this work.

References

1. Ahmadbeigi, N., A. Shafiee, E. Seyedjafari, Y. Gheisari, M. Vassei, S. Amanpour, S. Amini, I. Bagherizadeh, and M. Soleimani. Early spontaneous immortalization and loss of plasticity of rabbit bone marrow mesenchymal stem cells. *Cell Prolif.* 44:67–74, 2011.
2. Barron, V., K. Merghani, G. Shaw, C. M. Coleman, J. S. Hayes, S. Ansboro, A. Manian, G. O'Malley, E. Connolly, A. Nandakumar, C. A. van Blitterswijk, P. Habibovic, L. Moroni, F. Shannon, J. M. Murphy, and F. Barry. Evaluation of Cartilage Repair by Mesenchymal Stem Cells Seeded on a PEOT/PBT Scaffold in an Osteochondral Defect. *Ann. Biomed. Eng.* 43:2069–2082, 2015.
3. Brittberg, M. Cell carriers as the next generation of cell therapy for cartilage repair: a review of the matrix-induced autologous chondrocyte implantation procedure. *Am. J. Sports Med.* 38:1259–1271, 2010.
4. Chou, C.-L., A. L. Rivera, T. Sakai, A. I. Caplan, V. M. Goldberg, J. F. Welter, and H. Baskaran. Micrometer Scale Guidance of Mesenchymal Stem Cells to Form Structurally Oriented Cartilage Extracellular Matrix. *Tissue Eng. Part A* , 2012.doi:10.1089/ten.TEA.2012.0177

5. European Medicines Agency. MACI: EPAR Summary for the public. 2014.
6. Farr, J., B. J. Cole, S. Sherman, and V. Karas. Particulated articular cartilage: CAIS and DeNovo NT. *J. Knee Surg.* 25:23–29, 2012.
7. Freed, L. E., I. Martin, and G. Vunjak-Novakovic. Frontiers in tissue engineering. In vitro modulation of chondrogenesis. *Clin. Orthop.* S46–58, 1999.
8. Guilak, F., D. L. Butler, S. A. Goldstein, and D. Mooney. Functional Tissue Engineering. Springer, 2004, 452 pp.
9. Hababovic, P. Predictive Value of In Vitro and In Vivo Assays. In: Tissue Engineering, edited by J. P. Fisher. Springer, 2006.
10. Hurtig, M. B., M. D. Buschmann, L. A. Fortier, C. D. Hoemann, E. B. Hunziker, J. S. Jurvelin, P. Mainil-Varlet, C. W. McIlwraith, R. L. Sah, and R. A. Whiteside. Preclinical Studies for Cartilage Repair Recommendations from the International Cartilage Repair Society. *Cartilage* 2:137–152, 2011.
11. Hutmacher, D. W., K. W. Ng, C. Kaps, M. Sittinger, and S. Kläring. Elastic cartilage engineering using novel scaffold architectures in combination with a biomimetic cell carrier. *Biomaterials* 24:4445–4458, 2003.
12. Jansen, E. J. P., J. Pieper, M. J. J. Gijbels, N. A. Guldemond, J. Riesle, L. W. Van Rhijn, S. K. Bulstra, and R. Kuijer. PEOT/PBT based scaffolds with low mechanical properties improve cartilage repair tissue formation in osteochondral defects. *J. Biomed. Mater. Res. A* 89:444–452, 2009.
13. Jiang, W.-W., S.-H. Su, R. C. Eberhart, and L. Tang. Phagocyte responses to degradable polymers. *J. Biomed. Mater. Res. A* 82:492–497, 2007.
14. Johnstone, B., T. M. Hering, A. I. Caplan, V. M. Goldberg, and J. U. Yoo. In vitro chondrogenesis of bone marrow-derived mesenchymal progenitor cells. *Exp. Cell Res.* 238:265–272, 1998.

15. Jung, Y., S. H. Kim, S.-H. Kim, Y. H. Kim, J. Xie, T. Matsuda, and B. G. Min. Cartilaginous tissue formation using a mechano-active scaffold and dynamic compressive stimulation. *J. Biomater. Sci. Polym. Ed.* 19:61–74, 2008.
16. Jung, Y., M. S. Park, J. W. Lee, Y. H. Kim, S.-H. Kim, and S. H. Kim. Cartilage regeneration with highly-elastic three-dimensional scaffolds prepared from biodegradable poly(L-lactide-co-epsilon-caprolactone). *Biomaterials* 29:4630–4636, 2008.
17. Kavalkovich, K. W., R. E. Boynton, J. M. Murphy, and F. Barry. Chondrogenic differentiation of human mesenchymal stem cells within an alginate layer culture system. *In Vitro Cell. Dev. Biol. Anim.* 38:457–466, 2002.
18. Kelly, D. J., and P. J. Prendergast. Prediction of the optimal mechanical properties for a scaffold used in osteochondral defect repair. *Tissue Eng.* 12:2509–2519, 2006.
19. Lee, C. H., J. L. Cook, A. Mendelson, E. K. Moioli, H. Yao, and J. J. Mao. Regeneration of the articular surface of the rabbit synovial joint by cell homing: a proof of concept study. *Lancet* 376:440–448, 2010.
20. Løken, S., T. C. Ludvigsen, T. Høysveen, I. Holm, L. Engebretsen, and F. P. Reinholt. Autologous chondrocyte implantation to repair knee cartilage injury: ultrastructural evaluation at 2 years and long-term follow-up including muscle strength measurements. *Knee Surg. Sports Traumatol. Arthrosc. Off. J. ESSKA* 17:1278–1288, 2009.
21. Longo, U. G., S. Petrillo, E. Franceschetti, A. Berton, N. Maffulli, and V. Denaro. Stem cells and gene therapy for cartilage repair. *Stem Cells Int.* 2012:168385, 2012.

22. Makris, E. A., A. H. Gomoll, K. N. Malizos, J. C. Hu, and K. A. Athanasiou. Repair and tissue engineering techniques for articular cartilage. *Nat. Rev. Rheumatol.* 11:21–34, 2015.

23. Malda, J., T. B. F. Woodfield, F. van der Vloodt, C. Wilson, D. E. Martens, J. Tramper, C. A. van Blitterswijk, and J. Riesle. The effect of PEGT/PBT scaffold architecture on the composition of tissue engineered cartilage. *Biomaterials* 26:63–72, 2005.

24. Mendoza-Palomares, C., A. Ferrand, S. Facca, F. Fioretti, G. Ladam, S. Kuchler-Bopp, T. Regnier, D. Mainard, and N. Benkirane-Jessel. Smart Hybrid Materials Equipped by Nanoreservoirs of Therapeutics. *ACS Nano* 6:483–490, 2012.

25. Mooney, E., P. Dockery, U. Greiser, M. Murphy, and V. Barron. Carbon nanotubes and mesenchymal stem cells: biocompatibility, proliferation and differentiation. *Nano Lett.* 8:2137–2143, 2008.

26. Morrison, E. H., M. W. Ferguson, M. T. Bayliss, and C. W. Archer. The development of articular cartilage: I. The spatial and temporal patterns of collagen types. *J. Anat.* 189:9–22, 1996.

27. Moutos, F. T., L. E. Freed, and F. Guilak. A biomimetic three-dimensional woven composite scaffold for functional tissue engineering of cartilage. *Nat. Mater.* 6:162–167, 2007.

28. Ostrander, R. V., R. S. Goomer, W. L. Tontz, M. Khatod, F. L. Harwood, T. M. Maris, and D. Amiel. Donor cell fate in tissue engineering for articular cartilage repair. *Clin. Orthop.* 228–237, 2001.

29. Ponticiello, M. S., R. M. Schinagl, S. Kadiyala, and F. P. Barry. Gelatin-based resorbable sponge as a carrier matrix for human mesenchymal stem cells in cartilage regeneration therapy. *J. Biomed. Mater. Res.* 52:246–255, 2000.

30. Wang, K. Y., J. G. Horne, P. A. Devane, T. Wilson, and J. H. Miller. Chemical eluates from ultra-high molecular weight polyethylene and fibroblast proliferation. *J. Orthop. Surg. Hong Kong* 9:25–33, 2001.

Figure Captions

Figure 1 (A) Scanning electron microscopy image showing the top surface of the construct with circular pores, 180μm in diameter, (ii) the bottom surface with elliptical pores of dimensions of 200μm x 600μm and (iii) a cross section of the construct with pore size gradient increasing from the top to the bottom with a microtunnel through the construct highlighted in yellow. **(B)** Mechanical properties of the PLCL construct with (i) Stress strain curves generated for PLCL constructs in compression (n=5), (ii) Bar graph showing compressive stress at 50% strain, compressive modulus, and modulus of resilience. Values indicate means ± S.E.M.

Figure 2 Cytotoxicity using human MSCs as model for human application (i) Metabolic activity and (ii) cell number with MSC cultured in direct contact with the construct or using construct conditioned medium (elution) compared to cells cultured on tissue culture plastic as a control. Data is presented as mean ± SEM, n=3, $p>0.05$.

Figure 3 (A) Representative images of colony formation (i) in control culture medium or (ii) in culture medium with 2% rabbit serum (rabbit serum) demonstrating an increase in CFU-F in rabbit serum supplemented medium. **(B)** Number of colonies formed, revealing a statistically greater number of colonies formed in the presence of the rabbit serum **(C)** Growth of rabbit MSCs was significantly increased by the addition of 2% rabbit serum higher and **(D)** morphological images at passage 2 revealing that (i) larger flat cells with a senescent phenotype were visible in the absence of serum, as indicated by the black arrows, while (ii) cells cultured in the presence of rabbit serum have a typical fibroblastic appearance (scale bar 20 μm).

Figure 4 Representative images showing tri-lineage differentiation of rabbit MSCs. Cells induced to undergo adipogenesis showed reduced oil red O staining in the cells sub-cultured in the (i) absence of rabbit serum (rabbit serum) compared to (ii) cells sub-cultured in the presence of 2% rabbit serum (scale bar 200 μm). Calcium deposition indicative of osteogenesis, as detected by alizarin red staining, was also decreased in (iii) cells sub-cultured without rabbit serum compared to (iv) cells sub-cultured in the presence of 2% rabbit serum (scale bar 500 μm). There was no evidence of chondrogenesis observed in the (v) absence of rabbit serum, while positive toluidine blue staining for GAG was observed (vi) with rabbit serum (scale bar 200 μm).

Figure 5 H&E staining showing no adverse tissue response in terms of inflammation or giant cells in the empty defect, the cell-free construct or the rabbit MSC-seeded construct, at 4x, 10x and 20x objective lens magnification, with scale bar lengths of 1000 μm, 500 μm and 200μm respectively. Dotted black box shows original defect site areas and s denotes the scaffold.

Figure 6 (A) Toluidine blue staining showing absence of chondrogenesis in the empty defect and evidence of integration, GAG accumulation and chondrocytes in the cell-free PLCL construct. (4x, 10x and 20x objective lens magnification, with scale bar lengths of 1000 μm, 500 μm and 200μm respectively). Black arrows indicate areas of poor scaffold integration and s denotes the scaffold strut.

Figure 7 Collagen type II staining is positive in the adjacent tissue of the empty defect and in between and adjacent to the struts in the cell-free construct (brown DAB positive stain together with pink-eosin counterstain). The brown colour as evidence of collagen type II is less apparent in and around the struts of the cell-

seeded constructs at 4x and 20x objective lens magnification, with scale bar lengths of 1000 μm and 200μm respectively. Collagen type I staining is negative in the adjacent tissue (pink–eosin counterstain) and positive (brown) in the empty defect, in addition to the defects containing the cell-free construct and the rabbit MSC-seeded construct. Dotted box shows the outline of an empty defect, black arrows indicate the presence of collagen type II in the native tissue in the empty defect and the repair tissue in the scaffold containing defects. Red arrows indicate the absence of collagen type I in native cartilage and s denotes the PLCL strut.

Figure 1A Functionally graded pore size

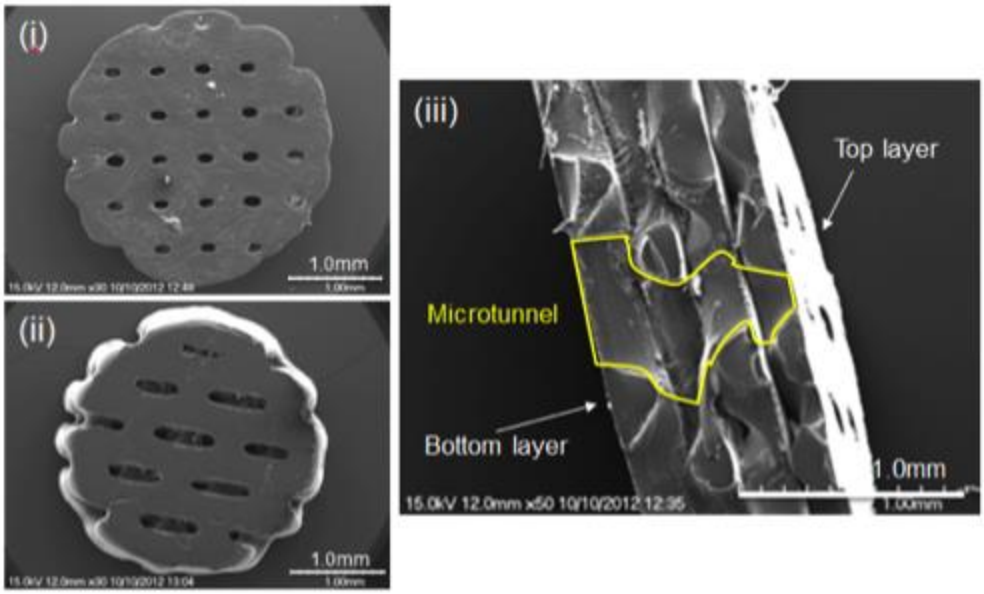

Figure 1B Compressive properties

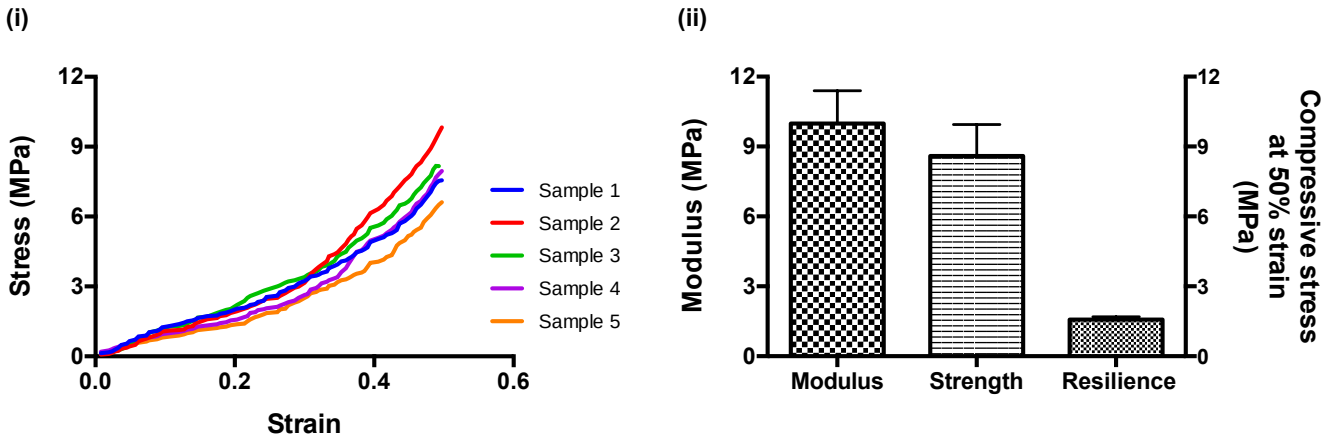

Figure 2 Cytotoxicity post sterilization

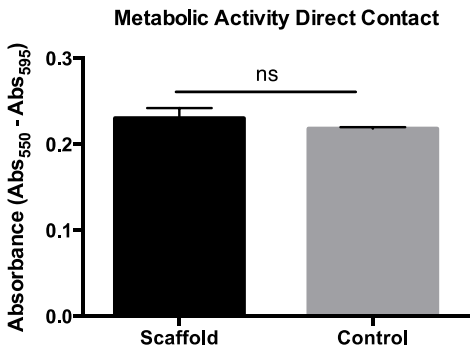

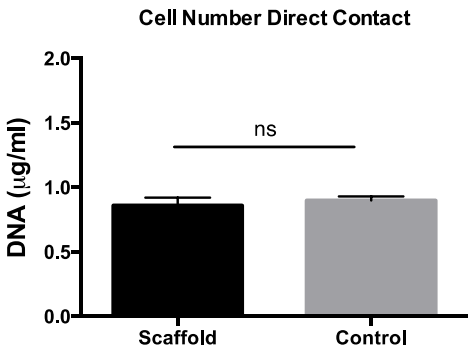

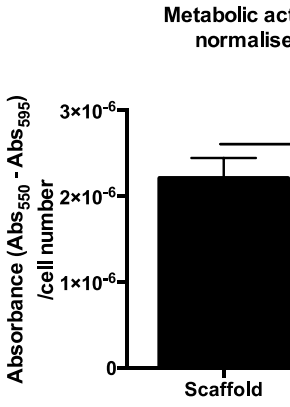

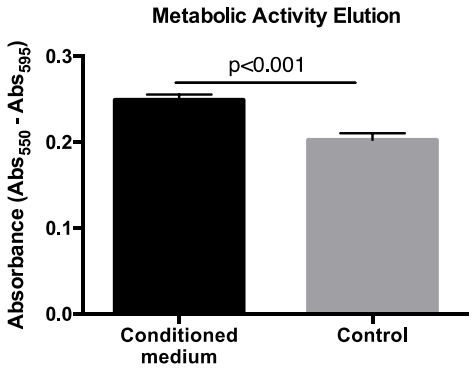

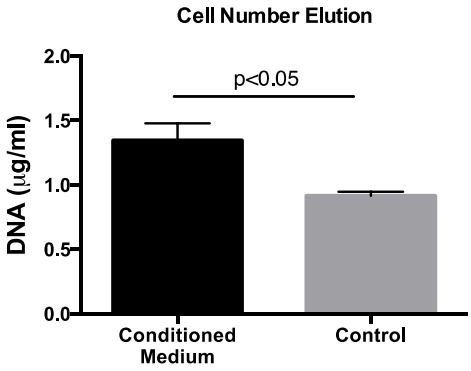

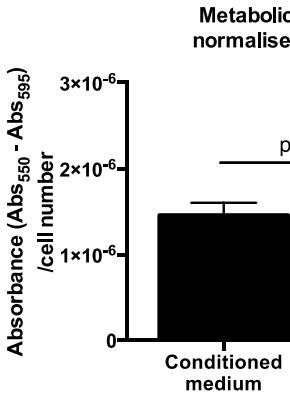

Figure 3 Isolation and characterisation of rabbit MSC

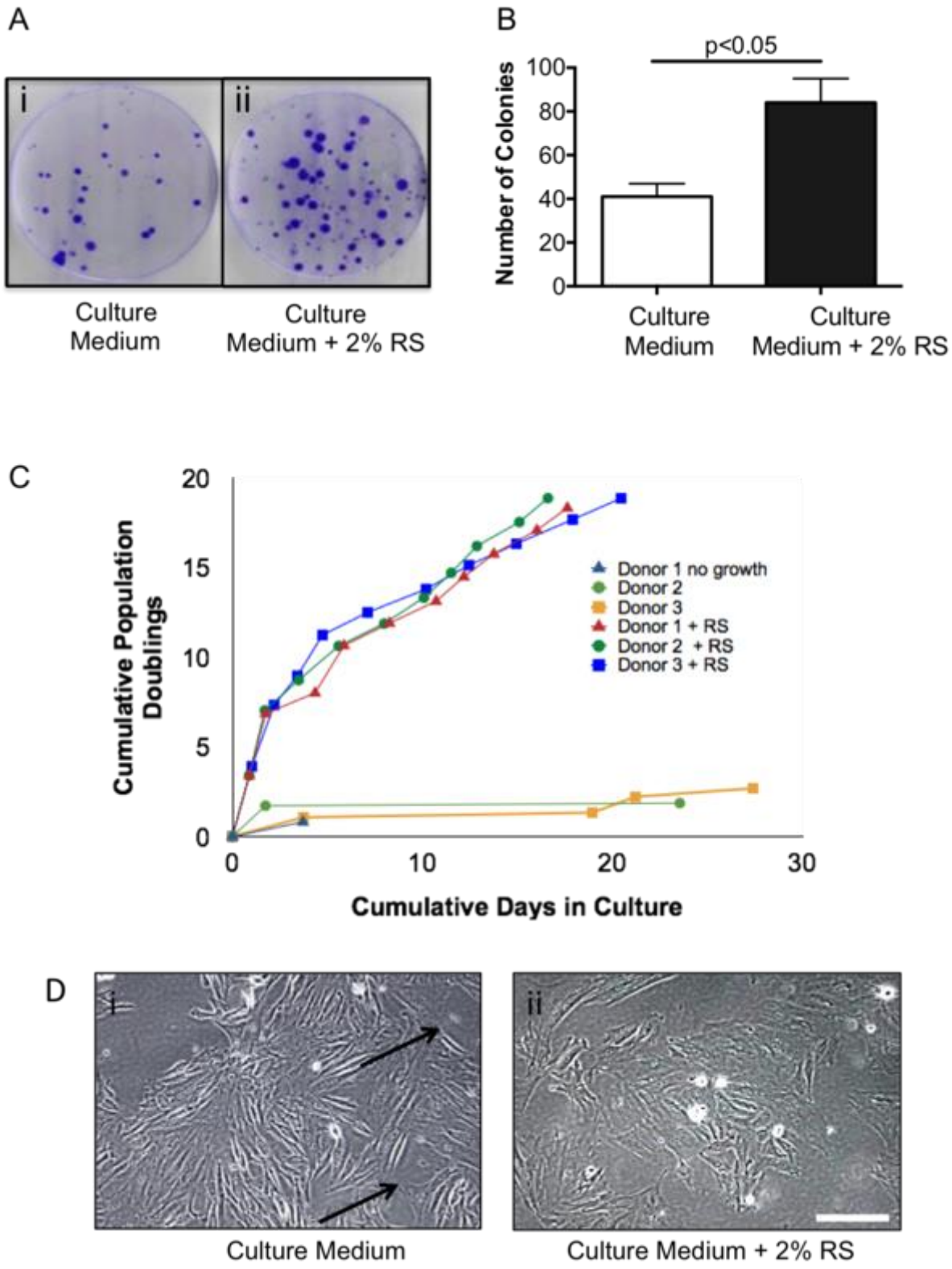

Figure 4 Tri-lineage differentiation of rabbit MSCs

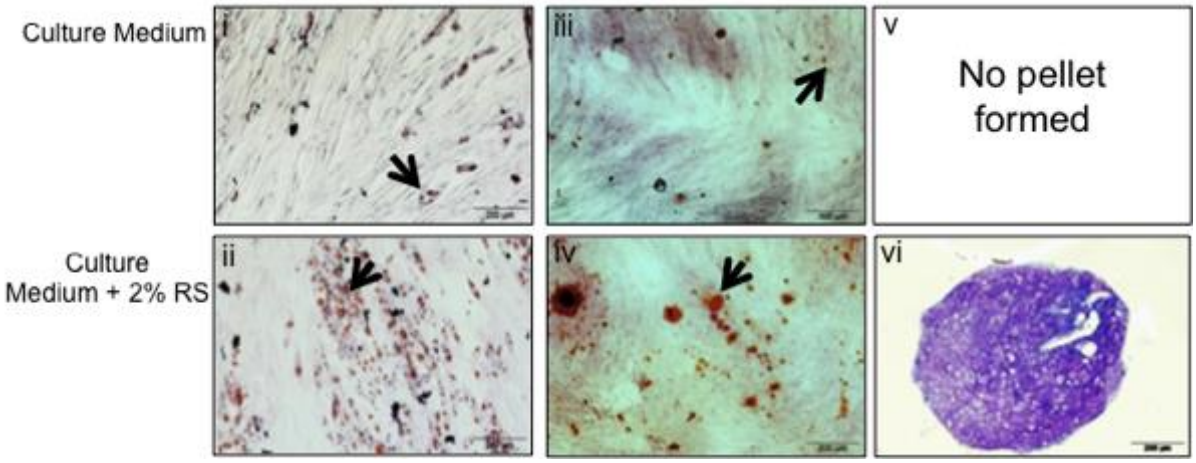

Figure 5 Histological evaluation: H&E staining

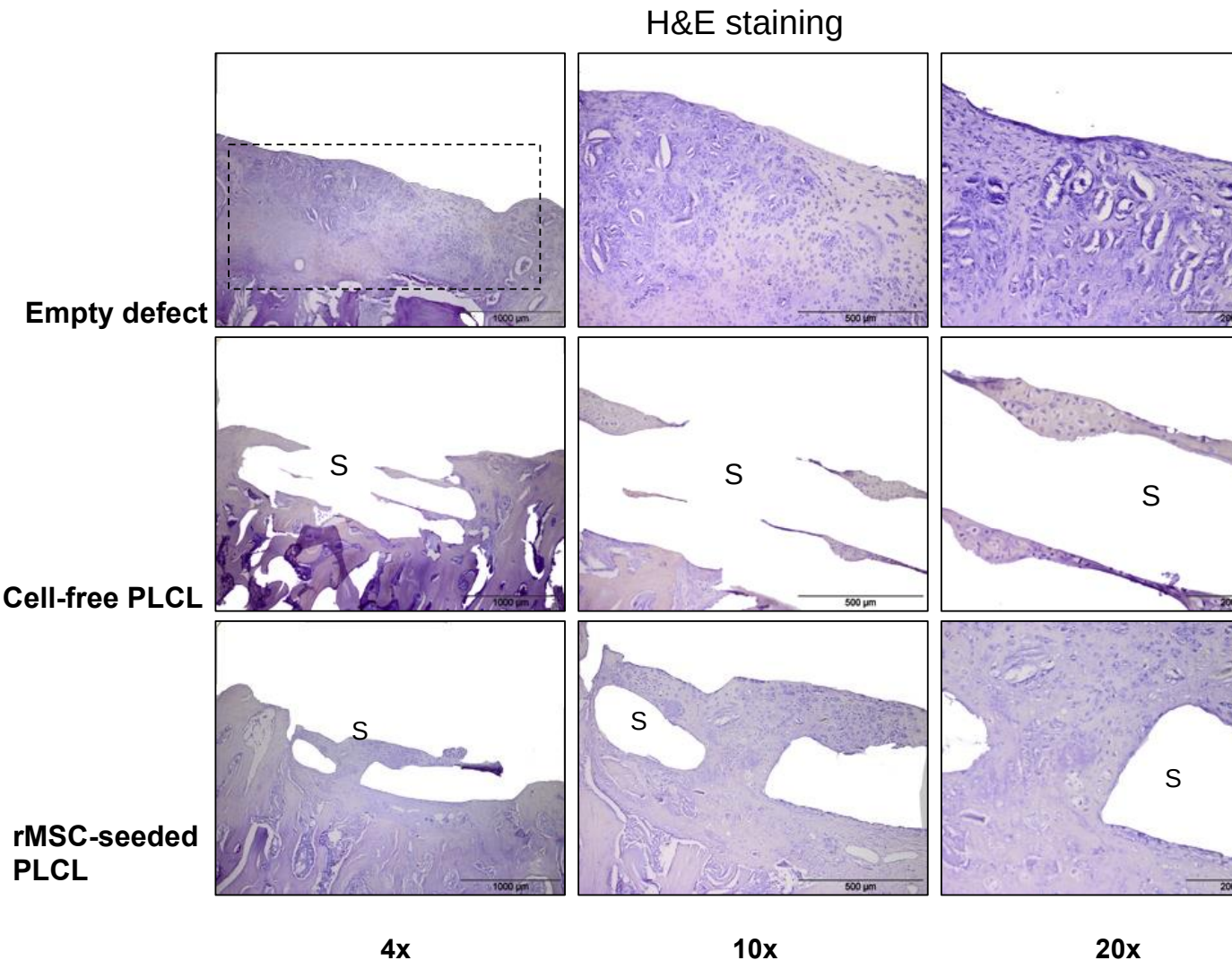

Figure 6 Histological evaluation: toluidine blue staining

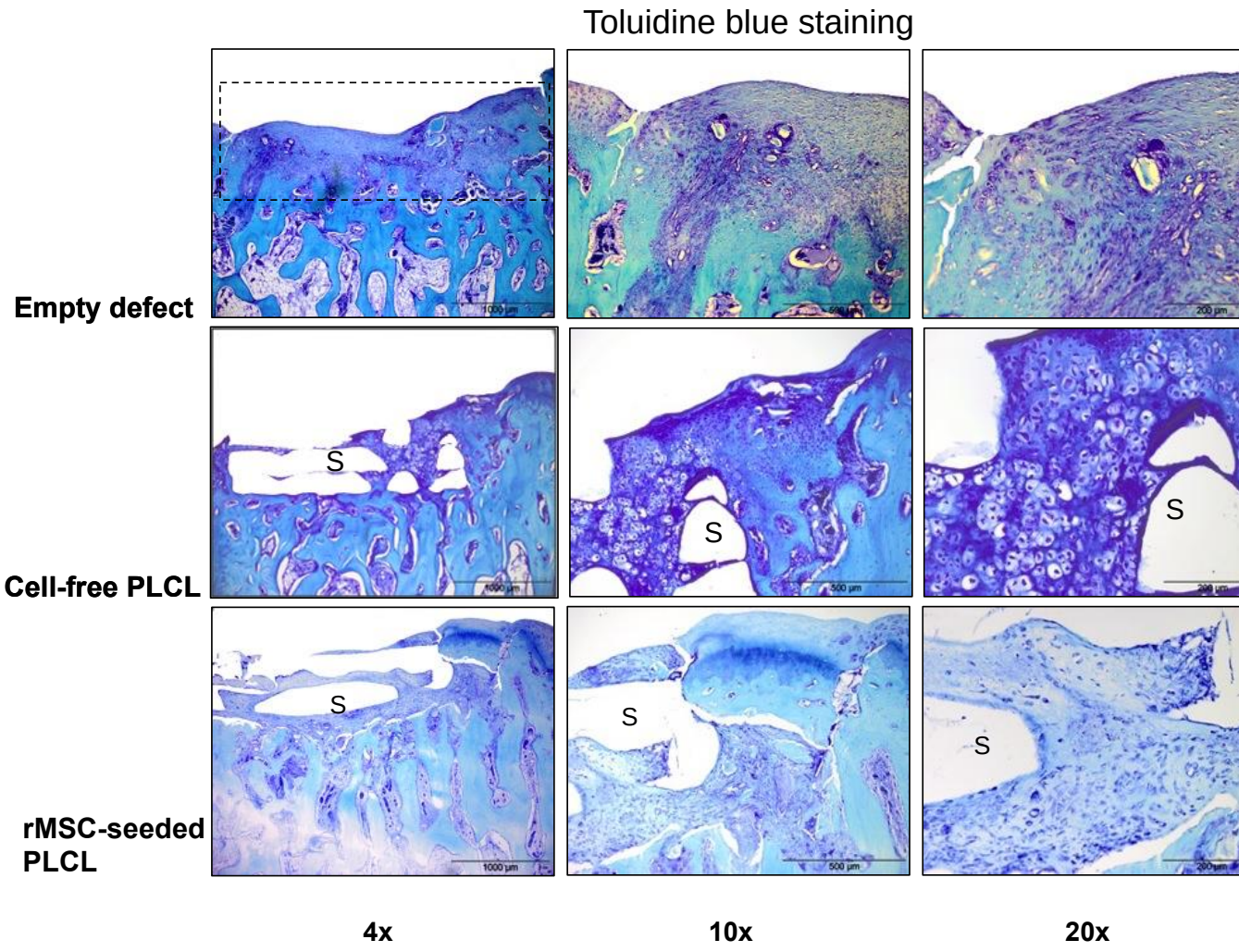

Figure. 7 Histological evaluation: Collagen type II and type I staining

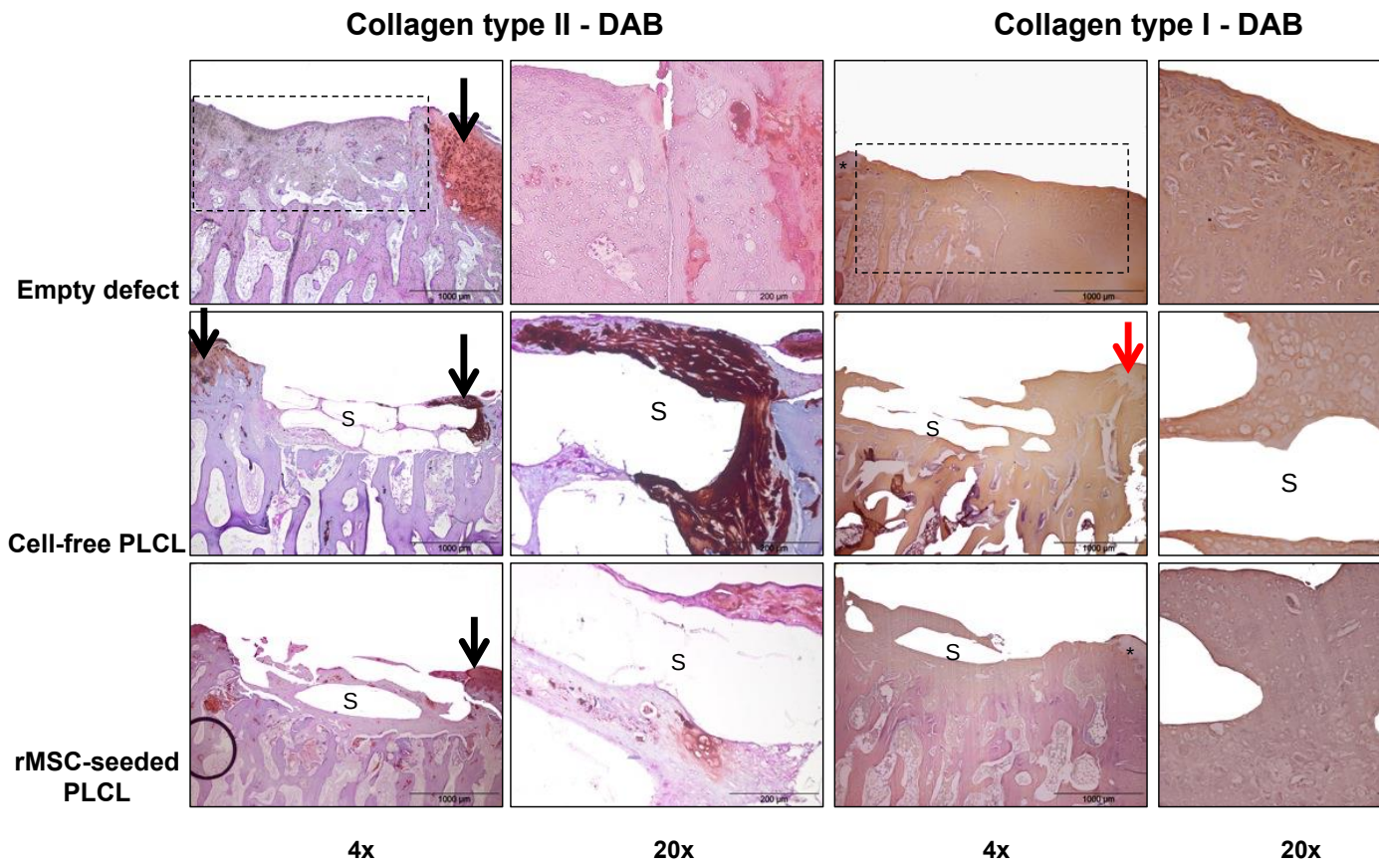

Supplementary information

Chemical properties after sterilization

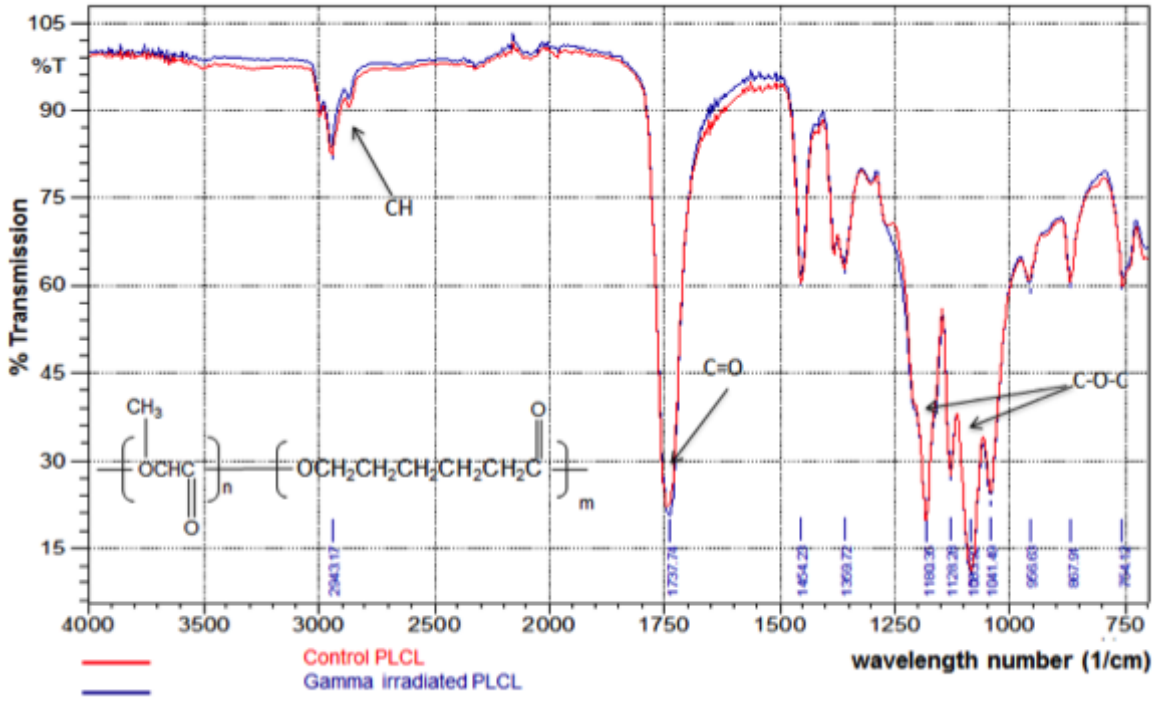

Thermal analysis of PLCL constructs

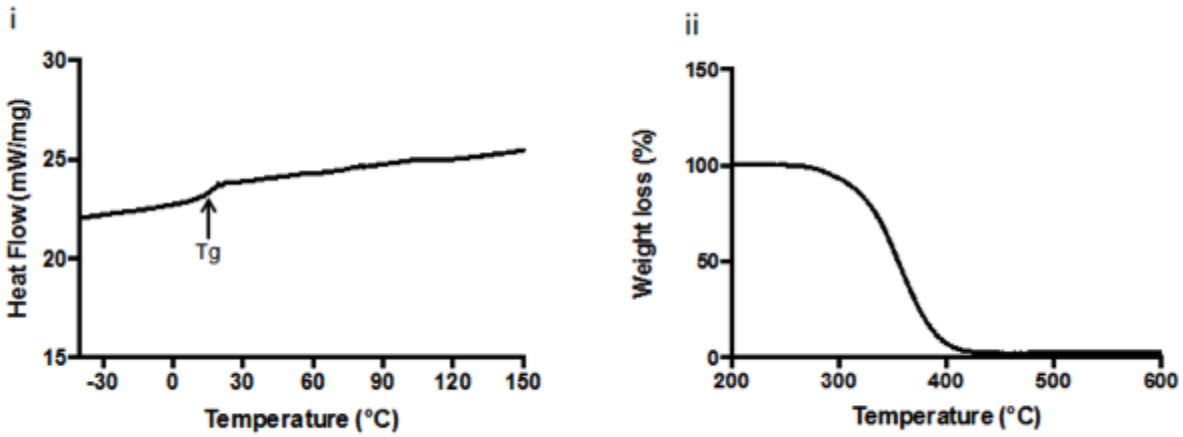

Molecular weight distribution of constructs

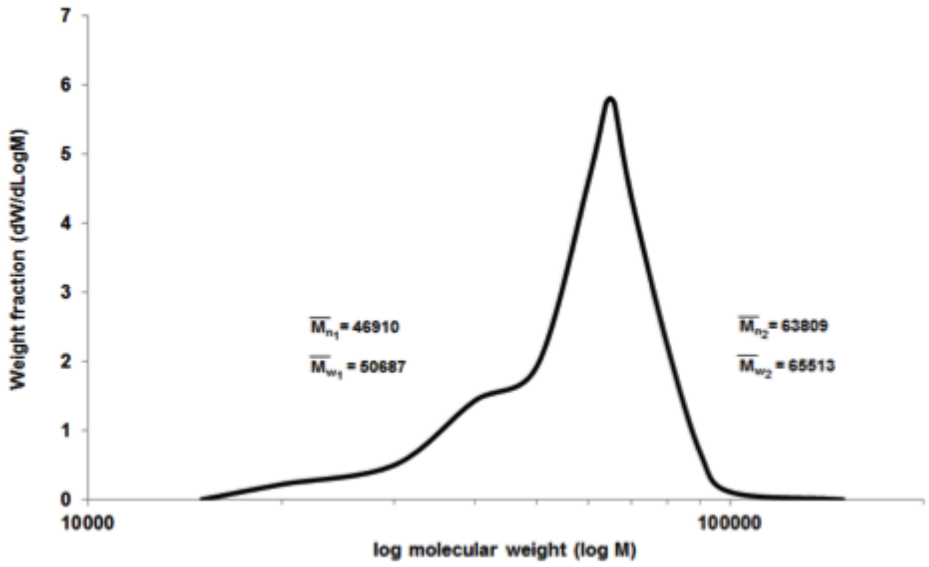

Montage of images stained with toluidine blue for all 18 defects (* indicate same rabbit).

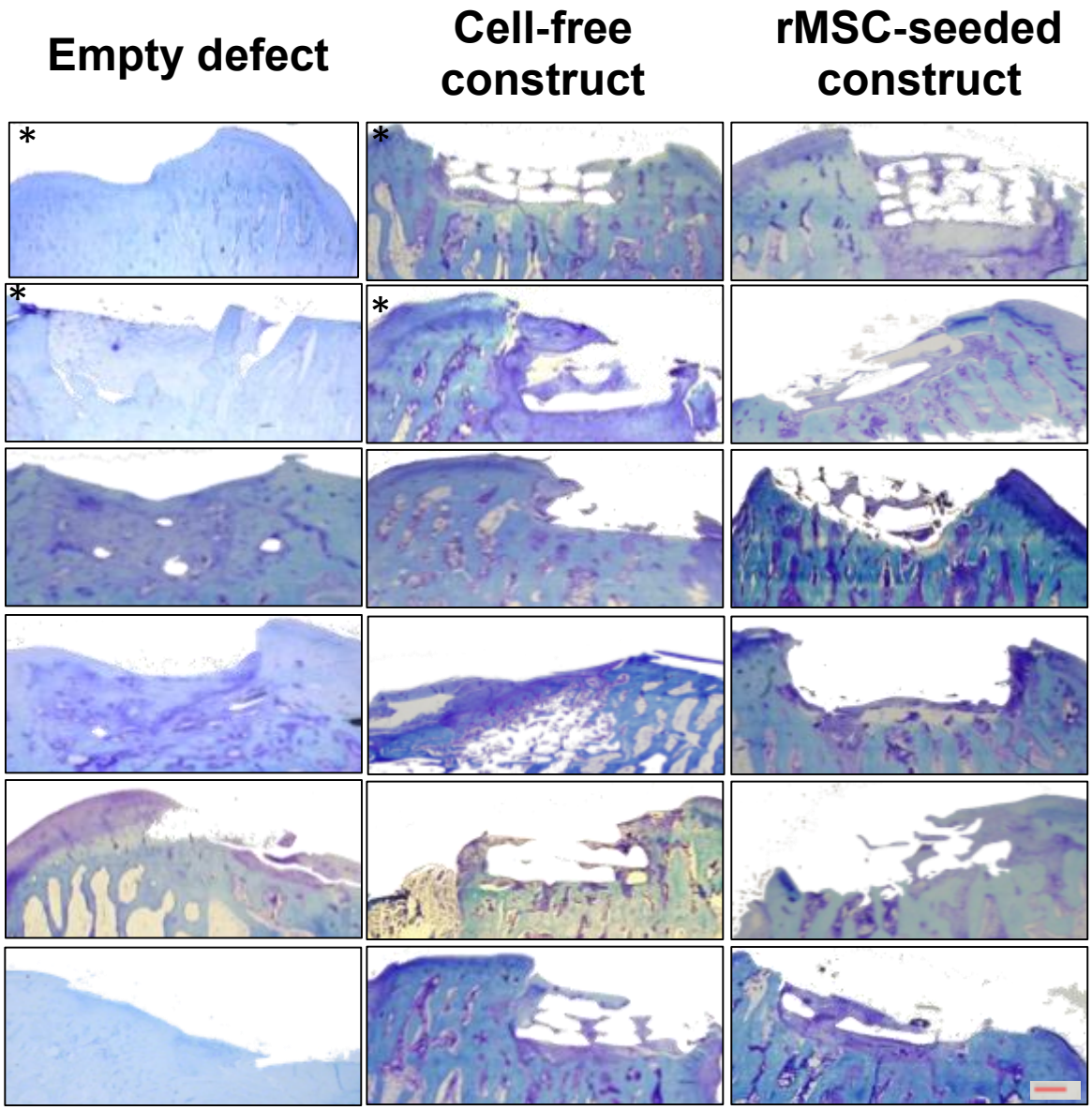

Video

Click here to download Video: Barron supplementary video.mov

Form for Disclosure of Potential Conflicts of Interest

Click here to download Form for Disclosure of Potential Conflicts of Interest: ocicmje-Valerie Barron.pdf

Form for Disclosure of Potential Conflicts of Interest

Click here to download Form for Disclosure of Potential Conflicts of Interest: ocicmje-Martin Neary.pdf

Form for Disclosure of Potential Conflicts of Interest

Click here to download Form for Disclosure of Potential Conflicts of Interest: coi_disclosure for annals of biomedical engineering KM Sept

Form for Disclosure of Potential Conflicts of Interest

Click here to download Form for Disclosure of Potential Conflicts of Interest: ocicmje-Sharon Ansboro.pdf

Form for Disclosure of Potential Conflicts of Interest

Click here to download Form for Disclosure of Potential Conflicts of Interest: ocicmje-Grace OMalley.pdf

Form for Disclosure of Potential Conflicts of Interest

Click here to download Form for Disclosure of Potential Conflicts of Interest: ocicmje-Georgina Shaw.pdf

Form for Disclosure of Potential Conflicts of Interest

Click here to download Form for Disclosure of Potential Conflicts of Interest: ocijme Niall Rooney.pdf

Form for Disclosure of Potential Conflicts of Interest

Click here to download Form for Disclosure of Potential Conflicts of Interest: Frank Barry ocicmje.pdf

Form for Disclosure of Potential Conflicts of Interest

Click here to download Form for Disclosure of Potential Conflicts of Interest: ocicmje-Mary Murphy.pdf